Title
What drives the seasonality of photosynthesis across the Amazon basin? A cross-site analysis of eddy flux tower measurements from the Brasil flux network

Authors
Restrepo-Coupe, Natalia
da Rocha, Humberto R
Hutyra, Lucy R
et al.

Publication Date
2013-12-01

DOI
10.1016/j.agrformet.2013.04.031

Agricultural and Forest Meteorology 182–183 (2013) 128–144

Contents lists available at ScienceDirect

Agricultural and Forest Meteorology

journal homepage: www.elsevier.com/locate/agrformet

What drives the seasonality of photosynthesis across the Amazon basin? A cross-site analysis of eddy flux tower measurements from the Brasil flux network

Natalia Restrepo-Coupe[a,b], Humberto R. da Rocha[c], Lucy R. Hutyra[e], Alessandro C. da Araujo[i,k], Laura S. Borma[o], Bradley Christoffersen[a], Osvaldo M.R. Cabral[j], Plinio B. de Camargo[b], Fernando L. Cardoso[r], Antonio C. Lola da Costa[p], David R. Fitzjarrald[f], Michael L. Goulden[l], Bart Kruijt[h], Jair M.F. Maia[i,d], Yadvinder S. Malhi[m], Antonio O. Manzi[i], Scott D. Miller[f], Antonio D. Nobre[i], Celso von Randow[h,s], Leonardo D. Abreu Sá[g], Ricardo K. Sakai[f], Julio Tota[i], Steven C. Wofsy[n], Fabricio B. Zanchi[q,t], Scott R. Saleska[a,*]

[a] *Department of Ecology and Evolutionary Biology, University of Arizona, Tucson, AZ 85721, USA*
[b] *University of Technology Sydney, Sydney, NSW 2007, Australia*
[c] *Department of Atmospheric Sciences, Universidade de São Paulo, São Paulo, Brazil*
[d] *Universidade do Estado do Amazonas (UEA), Manaus, Amazonas, Brazil*
[e] *Boston University, Department of Earth and Environment, Boston 02215, USA*
[f] *Atmospheric Sciences Research Center, State University of New York, Albany, NY, USA*
[g] *National Institute for Space Research (INPE), Belem, Para, Brazil*
[h] *Alterra, Wageningen University and Research Centre, Wageningen 6700, The Netherlands*
[i] *Instituto Nacional de Pesquisas da Amazônia (INPA), Manaus, Amazonas, Brazil*
[j] *Embrapa Meio Ambiente, Jaguariuna, Brazil*
[k] *Embrapa Amazônia Oriental, Belem, Para, Brazil*
[l] *Department of Earth System Science, University of California Irvine, Irvine, CA 92697, USA*
[m] *Oxford University Centre for the Environment, Oxford OX1 3QY, UK*
[n] *Division of Applied Sciences, Harvard University, Cambridge, MA 02138, USA*
[o] *Escola de Artes, Ciências e Humanidades, Universidade de São Paulo, São Paulo, Brazil*
[p] *Universidade Federal do Para, Belem, Brazil*
[q] *Vrije Universiteit Amsterdam, Amsterdam, The Netherlands*
[r] *Universidade Federal do Tocantins, Tocantins, Brazil*
[s] *Brazilian National Institute for Space Research, Center for Earth System Science, Cachoeira Paulista, SP, Brazil*
[t] *Universidade Federal do Amazonas (UFAM), Educação, Agricultura e Ambiente (IEAA), Manaus, Amazonas, Brazil*

ARTICLE INFO

Article history:
Received 3 August 2012
Received in revised form 22 February 2013
Accepted 16 April 2013

Keywords:
Tropical forest
Eddy covariance
Amazon
Seasonality
Ecosystem productivity
Cross-site

ABSTRACT

We investigated the seasonal patterns of Amazonian forest photosynthetic activity, and the effects thereon of variations in climate and land-use, by integrating data from a network of ground-based eddy flux towers in Brazil established as part of the 'Large-Scale Biosphere Atmosphere Experiment in Amazonia' project. We found that degree of water limitation, as indicated by the seasonality of the ratio of sensible to latent heat flux (Bowen ratio) predicts seasonal patterns of photosynthesis. In equatorial Amazonian forests (5° N–5° S), water limitation is absent, and photosynthetic fluxes (or gross ecosystem productivity, *GEP*) exhibit high or increasing levels of photosynthetic activity as the dry season progresses, likely a consequence of allocation to growth of new leaves. In contrast, forests along the southern flank of the Amazon, pastures converted from forest, and mixed forest-grass savanna, exhibit dry-season declines in *GEP*, consistent with increasing degrees of water limitation. Although previous work showed tropical ecosystem evapotranspiration (*ET*) is driven by incoming radiation, *GEP* observations reported here surprisingly show no or negative relationships with photosynthetically active radiation (*PAR*). Instead, *GEP* fluxes largely followed the phenology of canopy photosynthetic capacity (*Pc*), with only deviations from this primary pattern driven by variations in *PAR*. Estimates of leaf flush at three

* Corresponding author. Tel.: +1 520 6261500; fax: +1 520 621 9190.
E-mail addresses: nataliacoupe@gmail.com, nataliacoupe@yahoo.com (N. Restrepo-Coupe), saleska@email.arizona.edu (S.R. Saleska).

0168-1923/$ – see front matter
http://dx.doi.org/10.1016/j.agrformet.2013.04.031

non-water limited equatorial forest sites peak in the dry season, in correlation with high dry season light levels. The higher photosynthetic capacity that follows persists into the wet season, driving high *GEP* that is out of phase with sunlight, explaining the negative observed relationship with sunlight. Overall, these patterns suggest that at sites where water is not limiting, light interacts with adaptive mechanisms to determine photosynthetic capacity indirectly through leaf flush and litterfall seasonality. These mechanisms are poorly represented in ecosystem models, and represent an important challenge to efforts to predict tropical forest responses to climatic variations.

1. Introduction

The Amazon basin represents a major component of regional and global carbon and hydrological cycles. Globally significant variations in these cycles could be induced by climate change (Betts et al., 2004; Monteith, 1965), but predictions for the future of Amazon forests under climate change vary widely (Friedlingstein et al., 2006). Predictions of vegetation responses to long-term climate change are not easily tested, but common mechanisms also control response to short-term climatic variations, including seasonal variations. Thus, understanding seasonal and spatial variation of forest metabolism is an important basis for understanding ecological responses to climate generally. In contrast to temperate zones, where the seasonality of ecosystem metabolism is evident and straightforwardly dominated by the contrast between an active growing and a dormant season, the seasonality of photosynthetic activity of evergreen tropical forests is not so obvious.

The dominant seasonal rhythm in many Amazonian forests is that of rainfall, with a distinct dry season, when precipitation inputs fall below 100 mm month^{-1}, varying in length from 0 months (no dry season in the ever-wet northwestern Amazon) to 5 months in central eastern equatorial Amazonia, and in southwestern edge (Sombroek, 2001) (Fig. 1). The dry season brings a decrease in cumulus cloud cover and, in areas close to the equator with low variation in top-of-atmosphere solar energy, an increase in solar radiation at the surface. The dry season also brings increased smoke from biomass burning (Koren et al., 2004; Oliveira et al., 2007), shifting the composition of direct and diffuse radiation.

Many vegetation modeling studies have represented Amazon forests as water-limited, and so predicted dry season declines in transpiration and/or photosynthesis (Botta et al., 2002; Dickinson and Henderson-Sellers, 1988; Lee et al., 2005; Nobre et al., 1991; Tian et al., 1998). Early empirical studies near Manaus both supported (Malhi et al., 2002, 1998) and opposed (Shuttleworth, 1988) the water-limitation view. However, an accumulating suite of evidence is beginning to clarify the picture. Eddy flux measurements begun as part of the Large-scale Biosphere-Atmosphere Experiment in Amazonia (LBA) clearly show that evapotranspiration at some central Amazon sites is not water limited but largely driven by the availability of net radiation (da Rocha et al., 2004; Hutyra et al., 2007). Recently, integrated analysis across a network of towers confirms this behavior across much of the Amazon (Hasler and Avissar, 2007; Negrón Juárez et al., 2009; da Rocha et al., 2009; Fisher et al., 2009; Costa et al., 2010a,b). This evidence suggests that intact Amazon forests could be more resilient to variations in climate than most models have predicted. Deep tree roots (Nepstad et al., 1994) combined with hydraulic redistribution by roots (Oliveira et al., 2005) and increased availability of sunlight (Potter et al., 1998) have been suggested as explanations for these observations.

Remote sensing data from the moderate resolution imaging spectroradiometer (MODIS) suggest that intact forest photosynthesis increases as the dry season progresses across a large area of the central Amazon. The MODIS Leaf Area Index (*LAI*) product shows a widespread pattern of dry-season *LAI* increases that peak during the early to mid-dry season (Myneni et al., 2007), while the MODIS Enhanced Vegetation Index (*EVI*) shows equatorial Amazon forests continually "greening-up" throughout the dry season as availability of sunlight increases. By contrast, areas with extensive conversion of forests to pasture or agricultural management show the opposite "brown-down" trend (Huete et al., 2006). Remote sensing of regional-scale chlorophyll fluorescence (*Fs*) in the Amazon (by the new Japanese Greenhouse gases Observing SATellite, GOSAT, which may give a more direct index of photosynthesis than existing technologies (Frankenberg et al., 2011), suggests patterns broadly similar to those observed via EVI (*Fs* vs *EVI*, $R^2 = 0.52$) (Lee et al., 2013).

Tower-based estimates of photosynthetic flux derived from observations of net ecosystem exchange of carbon dioxide via eddy covariance method are perhaps the most reliable and direct measure of ecosystem scale photosynthesis to "ground truth" remote sensing indices and to test models. Individual tower studies have shown a range of results, including: (1) clear increases in dry season forest photosynthesis in the central eastern Amazon (Goulden et al., 2004; Hutyra et al., 2007; Saleska et al., 2003), (2) dry season decreases in the southwest Amazon (von Randow et al., 2004), and (3) no detectable seasonality in the far eastern Amazon (Carswell et al., 2002). These studies have pointed to a range of possible biophysical drivers for carbon assimilation, including length of dry season, cloud cover, access to deep water, and disturbance history, among others. Site-specific results suggest the need for a consistent, integrated analysis across sites and biomes of the seasonal patterns in eddy flux-derived ecosystem-scale photosynthesis to present a coherent picture of its spatial variability and possible drivers across the Amazon basin.

Our objective is to use eddy covariance (EC) data from a network of flux towers, installed as part of the 'Large-Scale Biosphere Atmosphere Experiment in Amazonia' (LBA) project (Keller et al., 2004), to address the question of what environmental and biological factors control the seasonality of photosynthesis in these tropical Amazonian ecosystem. We also sought to provide an integrated, consistently processed dataset, which could be used for comparison to model simulations of the LBA "Data-Model Intercomparison Project (LBA-DMIP). To this end, we conducted the first integrated analysis of basin-wide patterns of ecosystem photosynthesis across the Amazon. This effort is possible by the collaboration from a range of research groups who have contributed their observations to an integrated and unified database, known as Brasil flux network (da Rocha et al., 2009). The nine sites (Table 1) from this database are: four tropical forests and one converted pasture/agricultural site located along the main stem of the Amazon (equator to 3° S), one tropical dry forest and an adjacent converted site located in southern Amazonia (~10° S), one seasonally flooded ecotone (~10° S), and one non-Amazonian savanna in southern Brazil.

First, we describe the seasonal patterns of ecosystem photosynthetic fluxes, and canopy photosynthetic capacity across different Amazonian ecosystems, latitudinal gradients, and disturbance history. Then, we test hypotheses about control of photosynthesis by analyzing relationships between environmental drivers and overall photosynthetic fluxes and capacity. We initially focus on two main contrasting ideas drawn from the literature: that photosynthesis is limited by water availability, and that photosynthesis is limited by

Table 1
Brasil flux sites descriptions. The last two columns are the $u^*_{threshold}$ used for correcting for missing nighttime fluxes, and the method used for filling storage fluxes S_{co_2} when tower CO_2 profile measurements are missing (see text).

ID	Site name Lat/Lon.	Canopy height (m)	Biome type	Soil depth (m)	Water table depth (m)	LAI ($m^2\ m^{-2}$)	Measurement period	u^*_{thresh}. ($m\ s^{-1}$)[95% CI]	S_{co_2} filling method for GEP calculations
K34	Manaus 2.61S/60.21W	30–35	Tropical rainforest	>15 (Tomasella et al., 2007)	35	4.7 (Malhi et al., 2009)	14-Jun-99 to 30-Sep-06	0.20 [0.186–0.204]	Diel (Hutyra et al., 2008)
K67	Tapajos K67 2.85S/54.97W	35–40	Tropical rainforest	>12[h,k]	>100[b,j]	6.0[e]	2-Jan-02 to 23-Jan-06	0.266 [0.217–0.258]	No filling required
K83	Tapajos K83 3.01S/54.58W	35–40	Selectively logged tropical rainforest	>12[k]	>100[b,j]	4.9[f]	29-Jun-00 to 12-Mar-04	0.24 [0.233–0.303]	No filling required
CAX	Caxiuana 1.72S/51.53W	30–35	Tropical rainforest	3–4[h,l]	~10 wet season[l]	5.14[l]	1-Jan-99 to 30-Jul-03	0.22 [0.196–0.246]	Diel (Hutyra et al., 2008)
K77	Tapajos K77 2.42S/54.88W	0–0.6	Pasture-Agriculture (since Dec 2001)	>12[j,k]	>100[b,j]	2.52 (pasture) June 2001[g]	1-Jan-00 to 30-Dec-05	0.09 [0.076–0.101]	No filling required
RJA	Reserva Jaru 10.08S/61.93W	30	Tropical wet and dry forest	1 .2–4[a]	NA	5.5[a]	23-Mar-99 to 14-Nov-02	0.21 [0.195 0.219]	S_{co_2} based on a look up table, LUT
FNS	Fazenda Nossa Senhora 10.76S/62.36W	0.2–0.5	Pasture	7 [c]	~4.6 wet season ~6.3 dry season[c]	1,4 (2000) 2,8 (2003)[c]	4-Feb-99 to 4-Nov-02	0.13 [0.122 0.147]	$NEE \sim F_{co_2}$ low nighttime u^* corrected
JAV	Rio Javaes-Bananal Island 9.82S/50.13W	18 trees 5 understory	Seasonally flooded, forest-savanna ecotone	3[i]	3.7–4.5 1–5 mas (flooding)	3.5–4.5	24-Oct-04 to 8-Dec-06	0.15 [0.138–0.16]	S_{co_2} based on a look up table, LUT
PDG	Pe de Gigante 21.62S/47.63W	1–3 (73%) <8 (27%)[d]	Savanna (cerradao)	1–3 .5[i]	NA	6	1-Jan-04 to 31-Dec-06	0.34 [0.315–0.365]	$NEE \sim F_{co_2}$ low nighttime u^* corrected

Principle Investigators and data references (otherwise indicated at table):
K34: Manzi, A., Nobre, A. (INPA, Brazil) (Araújo et al., 2002a,b).
K67: Wofsy, S. (Harvard, USA), Saleska, S. (U of A, USA), Camargo, A. (CENA/USP, Brazil) (Hutyra et al., 2007; Saleska et al., 2003).
K83: Goulden M. (UC Irvine, USA), Miller, S. (SUNY, Albany, USA), da Rocha, H. (USP, Brazil) (da Rocha et al., 2004; Goulden et al., 2004; Miller et al., 2004).
CAX: Sa, L. (Museo Goeldi), da Rocha, H. (USP, Brazil) (Carswell et al., 2002; Souza Filho et al., 2005).
K77: Fitzjarrald, D. (SUNY, Albany, USA) (Sakai et al., 2004).
RJA: Manzi, A. (INPA, Brasil), Cardoso, F. (UFR, Brazil) (Kruijt et al., 2004; von Randow et al., 2004).
FNS: Manzi, A. (INPA, Brazil) (von Randow et al., 2004).
JAV: da Rocha, H. (USP, Brazil) (Borma et al., 2009).
PDG: da Rocha, H. (USP, Brazil) (da Rocha et al., 2002).

[a] Andreae et al. (2002).
[b] Nepstad et al. (2002).
[c] Zanchi et al. (2009).
[d] Fidelis and Godoy (2003).
[e] Domingues et al. (2005).
[f] Doughty and Goulden (2008).
[g] Negrón Juárez et al. (2009).
[h] Described as free of hardpan or iron oxide concretions.
[i] Personal communication.
[j] Assumed to be similar to nearby study sites.
[k] Oliveira et al. (2005).
[l] Malhi et al. (2009).

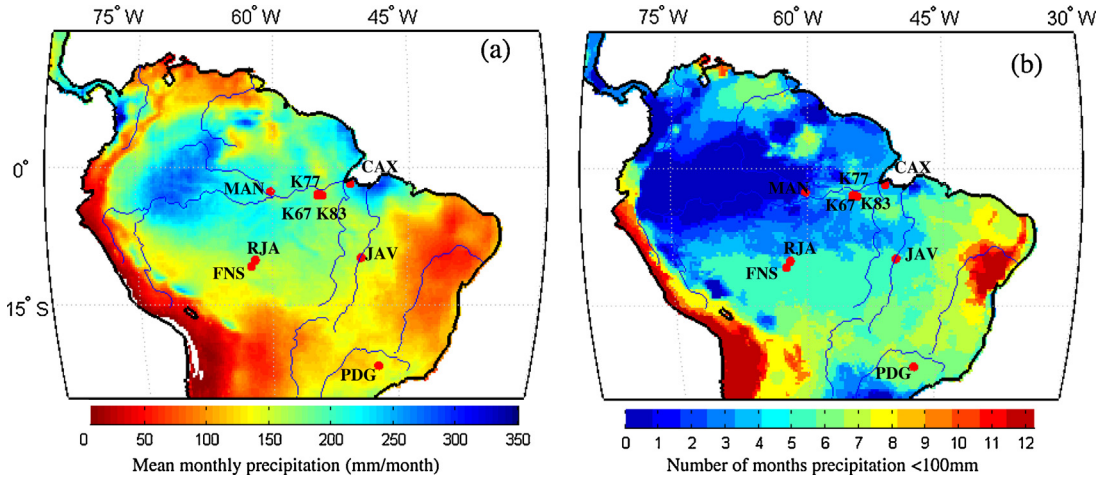

Fig. 1. (a) Average monthly (1998–2012) precipitation (mm month^{-1}) at the Amazon region according to Tropical Rainfall Measuring Mission (TRMM). Location of Brasil flux network sites: Santarém forests (K67 and K83), Santarém converted site (K77), Manaus forest (K34), Caxiuanã forest (CAX), Reserva Jarú southern forest (RJA), Fazenda Nossa Senhora southern converted site (FNS), Javés River-Bananal Island (JAV) and savanna Pe-de Gigante (PDG). (b) Number of dry months per year, defined as monthly precipitation less than 100 mm.

available energy. Finally, after finding that photosynthetic seasonality is not well-explained by environmental variables alone, we advance the hypothesis that it arises instead from the interaction between biologically determined leaf phenology and environmental drivers. We explore this third hypothesis with a simple model of canopy phenology that assumes photosynthetic capacity arises from the balance between loss of capacity to litterfall and increase of capacity from new leaf-flush.

2. Materials and methods

2.1. Site descriptions

We compiled original flux data from nine LBA eddy covariance towers in the Brazil flux network (Fig. 1 and Table 1). From east to west and north to south, these sites are: the Reserva Cuieiras near Manaus (K34 forest), the Tapajós National forest, near Santarém (K67 and K83 forests, and K77 pasture/agriculture), the Caxiuanã National forest near Belém (CAX forest), the Reserva Jarú (RJA forest) and Fazenda Nossa Senhora (FNS pasture), near Ji-Paraná-Rondônia, the Tocantins-Javaes site (JAV seasonally flooded ecotone) on Bananal Island, and the Reserva Pe-de-Gigante in Sao Paulo state (PDG savanna).

The equatorial forest sites are located near the main stem of the Amazon River, close to the equator (~3° S). The Manaus K34 forest tower is the westernmost of the equatorial Amazonian sites, located 60 km north of the city of Manaus (Araújo et al., 2002a). Santarém tropical moist forest towers (K67 and K83) are near the confluence of the Tapajós and Amazon rivers, midway between Manaus and the Atlantic coast. Santarém K77 was a forest area converted to pasture (~1990) and later (November 2001) was burned and plowed, followed by planting of non-irrigated rice (February 2001), and other crops (Keller et al., 2004; Sakai et al., 2004; Wick et al., 2005). Caxiuanã National Forest, (CAX) is a dense lowland forest located close to the Baia de Caxiuanã and the city of Belém (Pará) North-Eastern Brazil (Carswell et al., 2002).

Southern Amazon sites include Reserva Jarú (RJA), a tropical wet and dry (Peel et al., 2007) forest located in the state of Rondônia (Brazil) latitude ~ 10° S, 100 km north of Ji-Paraná. Fazenda Nossa Senhora da Aparecida (FNS) is a cleared forest, pasture close to the RJA forest tower, located on the Igarapé Lourdes Indian Reservation, which is about 30 km northwest of the city of Ji-Paraná (Gu et al., 2001; von Randow et al., 2004). The Bananal Island site (JAV) is a seasonally flooded (forest-savanna) ecotone, located on the state of Tocantins close to the Javaes River (Borma et al., 2009). Finally, south of the Amazon basin proper, is Reserva Pe-de-Gigante, in Sao Paulo state (PDG), also known as Sao Paulo-cerrado, a tropical woodland savanna site (da Rocha et al., 2002).

An analysis by Rosolem et al. (2008) showed that climatic and weather patterns at each site during the periods of flux observation (Supplement Table 1 and Fig. 2), were generally representative of the long-term climatology of each site, in particular: (1) precipitation was statistically consistent with the climatology and (2) temperature showed a slight tendency (not statistically significant) toward higher values. Only temperature at the seasonally inundated site (JAV) was ~1 °C higher than climatology.

Mean monthly Amazon basin precipitation (Fig. 1) is 182 mm month^{-1} with a range from 75 to 304 mm month^{-1}, based on the Tropical Rainfall Measuring Mission (TRMM) data product from 1998–2010 (3B43-v7 derived by combining TRMM satellite data, GOES-PI satellite data, and a global network of gauge data) (NASA, 2010). The spatial and temporal patterns of Amazon rainfall are associated with the behavior of the Intertropical Convergence Zone (ITCZ) centered over the Basin December to February (Horel et al., 1989). At the southern Amazon sites, the start of the dry season falls in the range of March to May as the ITCZ moves toward the NW (Central America) where it remains ~June to September.

The equatorial Amazon (5° S–5° N) seasonal dry period induces a peak in maximum incoming solar radiation. A defined dry season (<100 mm month^{-1}) is absent in the NW corner of the basin, where we observe the highest annual precipitation values (mean monthly precipitation > 250 mm) (Fig. 1). Toward the south (>5° S), the onset of the dry season (when cloud cover is low) is in May and extends until the end of Aug, out of phase with the period of highest top of the atmosphere radiation (Jul to Sep, depending on latitude). At these southern sites, the onset of the wet season thus coincides with the increase of top-of-atmosphere incoming radiation (TOA).

2.2. Net and gross ecosystem exchange (NEE and GEE) of CO_2 fluxes

Sites in the Brasil flux network used the eddy covariance (EC) method to measure the turbulent fluxes of CO_2 (F_{co_2} in μmol CO_2 m^{-2} s^{-1}), sensible (H in W m^{-2}) and latent heat (LE in W m^{-2}), and momentum (τ in kg m^{-1} s^{-2}). For a detailed site description,

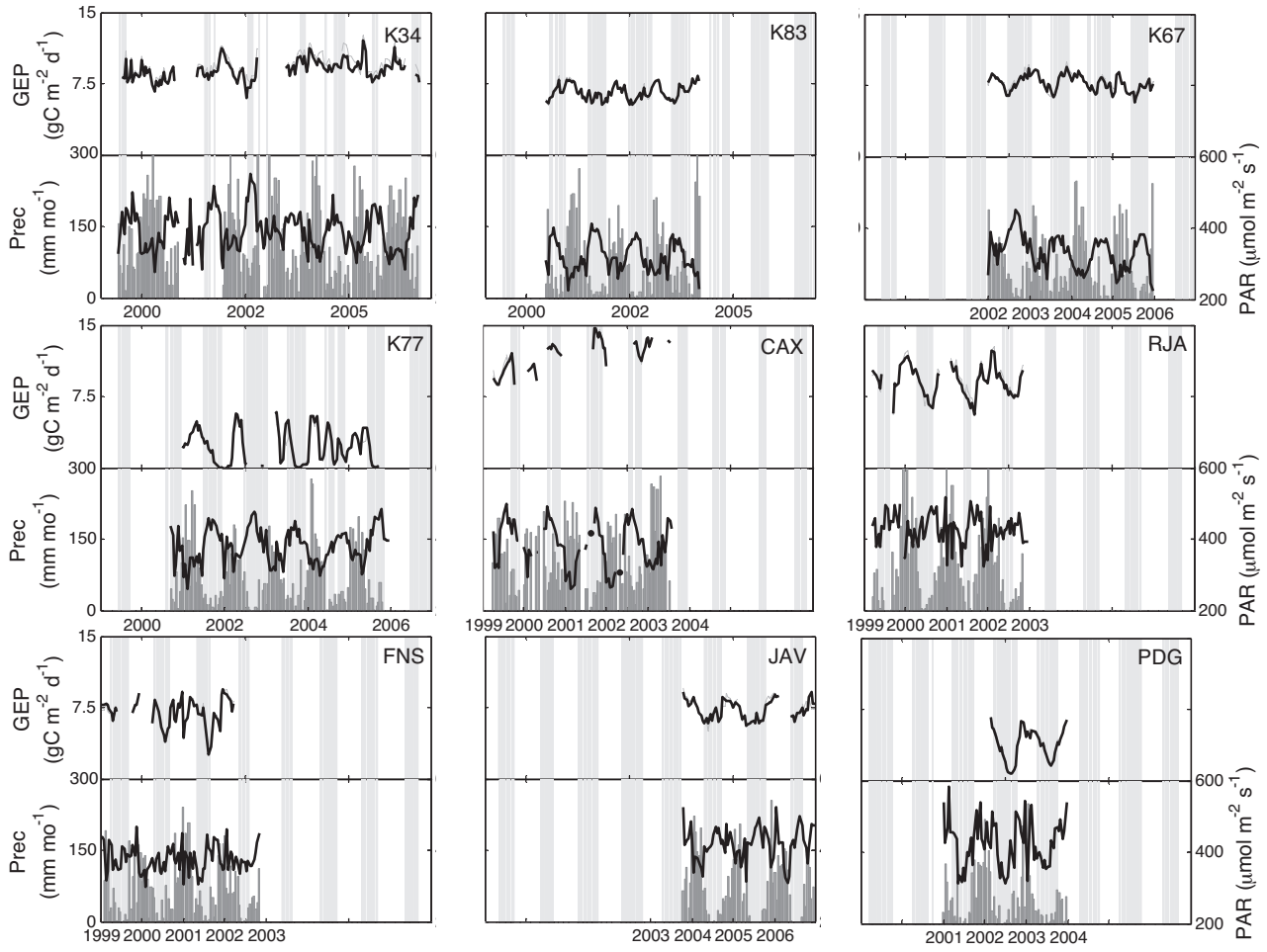

Fig. 2. Time series (16-day composites) of gross ecosystem productivity (*GEP*, in gC m^{-2} d^{-1}) (top panel for each site), upper and lower gray lines correspond to *GEP* calculated using minimum and maximum $u^*_{threshold}$ bound values; and daytime photosynthetic active radiation (*PAR*, in µmol m^{-2} s^{-1}) and Precipitation (*Prec*, in mm $month^{-1}$) (bottom panel for each site). Gray shaded areas indicate dry seasons (defined as periods with precipitation less than 100 mm $month^{-1}$), based on Tropical Rainfall Measuring Mission (TRMM) data.

instrumentation type and basic methods for processing the raw eddy-flux high frequency data and aggregation to hourly intervals, refer to the site-specific references and information listed in Table 1 and Supplement Table 2, and previous work by Keller et al. (2004), da Rocha et al. (2009) and Saleska et al. (2009).

Starting with half-hourly data provided from each site's operators, we calculated net ecosystem exchange (*NEE* in µmol CO_2 m^{-2} s^{-1}, with fluxes to the atmosphere defined as positive) as the sum of turbulent eddy flux above the forest (F_{co_2}) and the time rate of change in CO_2 stored within the canopy (the "storage flux", S_{co_2}) (Wofsy et al., 1993).

Some forest sites had instrument malfunctions that prevented the acquisition of storage flux (S_{co_2}) measurements for long periods, and we corrected for missing storage in these cases by using one of three methods for estimating the storage flux, as described in Restrepo-Coupe et al. (in preparation), and summarized here in Table 1. It is well known that when significant CO_2 can accumulate in the canopy airspace (as in forests) the absence of storage fluxes prevents accurate characterization of diel patterns of CO_2 exchange (Wofsy et al., 1993; Iwata et al., 2005). Similarly, S_{co_2} is in some cases important when determining seasonal patterns of *NEE* and its components. This is because the magnitude of S_{co_2} is inversely correlated with the strength of turbulent mixing (e.g. as measured by friction velocity u^*), and turbulence mixing varies seasonally. We believe that our correction for missing storage data is adequate for the purposes of comparing seasonal patterns across sites. However, several of the forest sites in this analysis suffered from long gaps in storage data, especially at Caxiuanã, and our findings for this site are therefore less robust.

Next, we quality-checked and aggregated *NEE* and environmental driver data to an hourly time-step. For quality control and assurance, we used the energy balance equation to help us identify outliers in CO_2, H_2O and sensible heat fluxes (F_c, *LE*, and *H*, respectively). We treated data as unreliable and removed it from the dataset when energy flux residuals were greater than 3-standard deviations away from the linear regression ($Rn = LE + H$, where *Rn* is the net radiation in W m^{-2}). Similarly, we filtered data for consistency between sonic anemometer and infrared gas analyzer measurements, on the one hand, and meteorological data (air temperature and water vapor concentration from HMP45 sensors, and wind speed from cup anemometers).

We removed isolated observations that were preceded and followed by a missing value. Any residual spikes from the hourly *NEE* data were identified, following the method proposed by Papale et al. (2006) and modified by Barr et al. (2009).

Because *NEE* can be erroneously low when turbulence is low, and because nighttime turbulence often varies seasonally, failure to correct for low turbulence could introduce a seasonal bias. We

therefore followed the standard practice (Aubinet, 2008) of correcting nighttime hourly *NEE* values for periods of low turbulent mixing by filtering out periods when friction velocity (u^* in m s^{-1}) was below a threshold value (u^*_{thresh}), and filling those times with estimates averaged from nearby valid measurements (those taken during periods that had more vigorous mixing). We filled each nighttime missing value from an average of all valid nighttime values within a 5-day window. If there were less than 36 valid hourly values within the window, the window was expanded until 36 valid points were encompassed (to a maximum window size of 30 days).

Site-specific u^*_{thresh} values were calculated by dividing the dataset into three-month intervals and for each interval creating a look up table (LUT) of nighttime *NEE* as a function of seven air temperature (T_a) bins of equal u^* (m s^{-1}) sample size (see Restrepo-Coupe et al., in preparation). The selected u^*_{thresh} was chosen as the lowest u^* bin for which corresponding *NEE* (averaged across temperature bins) was at least 99% of the maximum *NEE* bin average (Barr et al., 2009; Papale et al., 2006).

At the K77 pasture/agricultural site near Santarém, we used *NEE* values calculated from a nocturnal accumulation method (Sakai et al., 2004) without applying u^* correction per se, as calm nights were the norm at this ecosystem (pastures have lower turbulence compared to forests) and previous analysis showed that even with u^* filtering, nighttime *NEE* was underestimated (Sakai et al., 2004). There are no CO_2 storage measurements for the two non-forest sites, FNS (pasture) and PDG (savanna); here we assumed *NEE* is equivalent to F_{co_2}.

We derived gross ecosystem exchange (*GEE*) from tower measurements of daytime *NEE* by subtracting estimates of ecosystem respiration (R_{eco}), which in turn we derived from the u^*_{thresh} filtered nighttime *NEE* (Goulden et al., 2004; Hutyra et al., 2007; Saleska et al., 2003). We did not use a temperature function to extrapolate nighttime *NEE* to daytime R_{eco}, as is done at some higher latitude sites (Goulden et al., 1996), because we did not observe any within-month correlation between nighttime hourly *NEE* and nighttime T_a at any of the sites. Assuming daytime R_{eco} is the same as nighttime R_{eco} may underestimate the magnitude of daytime R_{eco} (and hence, of *GEE*) if R_{eco} is temperature sensitive, but we believe that any such underestimation will have little effect on the seasonal pattern, which is the focus here. Hourly R_{eco} is calculated as the average of valid nighttime *NEE* within a centered 5-day wide window, assuming at least 36 valid hours of nighttime *NEE* were available. If not, we expanded the window from 5 days until sufficient valid data were included (up to 31 days).

As defined above, *GEE* is a negative value ($GEE = NEE + R_{eco}$, with *NEE* negative in the daytime, and R_{eco} positive); we express ecosystem-scale photosynthesis, or Gross Ecosystem Productivity (*GEP*), as a positive value by equating it to negative *GEE*. *GEP* is equal to negative *GEE* assuming negligible leaf re-assimilation of dark respiration and insignificant CO_2 recirculation within the canopy air space, below the EC system (Stoy et al., 2006). Missing *GEP* data is filled using a look up table, calculated for a moving window of 11–21 or 31 days (with window size set to achieve a minimum of 16 h of valid data), of mean *GEP* compared to photosynthetic active radiation (*PAR*), divided into bins of width 200 μmol m^{-2} s^{-1}) and time of day (2-h wide bins). The hourly bins account for the higher sensitivity of photosynthetic activity to light in the morning compared to afternoon (Goulden et al., 2004) and the moving window accounts for sensitivity to seasonally varying soil moisture.

We aggregated hourly *GEP* to 16-day time periods for purposes of presentation, assuming that at least 4 days were available with at least 21 h of observations each (Fig. 2). Gaps were not filled further. The ~16-day window is a time scale representative of important ecological processes, in particular, leaf appearance to full expansion (Jurik, 1986) and corresponds to the MODIS vegetation index product interval.

2.3. Canopy photosynthetic capacity and Bowen ratios

Pc is an index of canopy photosynthetic capacity that is independent of varying light levels; we estimate it as the mean ecosystem productivity (*GEP*) for a fixed range of *PAR* ($725 < PAR < 925$ μmol m^{-2} s^{-1}), following Hutyra et al. (2007).

Pc is closely related to canopy-scale Light Use Efficiency (*LUE*), since dividing by the fixed *PAR* level for which it is defined (~825 μmol m^{-2} s^{-1}) gives the average slope of the light response curve in units of *LUE* (e.g. μmol CO_2 fixed per μmol *PAR*). It is also significantly correlated (R~0.47, $p < 0.0005$) with seasonal patterns in *LAI* (as measured optically by an LAI-2000 instrument) an independently derived index of photosynthetic infrastructure (Supplement Fig. 5).

Canopy-scale photosynthetic capacity arises from factors in addition to *LAI* (including variations in photosynthetic capacity at the leaf scale), but the correlation with *LAI* confirms that *Pc* is in fact capturing not just flux but underlying infrastructure. Interpretation of *Pc* strictly as an index of canopy-scale photosynthetic infrastructure that is independent of environmental conditions may still be confounded by the covarying seasonality of other environmental factors, in particular, vapor pressure deficit (*VPD*). *VPD* should be higher in the dry season, and higher *VPD* should induce stomatal closure that suppresses canopy photosynthesis at any given light level (Lasslop et al., 2010; Lloyd and Farquhar, 2008; Wehr et al., 2013). We therefore compared our results, where possible, to a version of *Pc* defined for different fixed *VPD*-bins to test the effect of removing *VPD* changes on the results (see Section 3.3).

In this analysis, we refer to normalized values for *GEP* and *Pc*, dividing by the maximum value within the annual cycle to give, $GEP\ GEP_{max}^{-1}$ and $Pc\ Pc_{max}^{-1}$, as our focus here is on investigating differences in seasonal patterns across sites, not on the absolute differences in carbon balance, which may be less certain. For the 16-day intervals, *GEP* and *Pc* were calculated in units of gC m^{-2} d^{-1}.

Evapotranspiration (*ET*) and photosynthetic activity (*GEP*) are considered tightly related processes and both fluxes will decrease during periods of water stress or low incoming radiation and ambient temperatures. As an indicator of water stress, we calculated the Bowen ratio of sensible (*H*) to latent heat flux (*LE*), similar to Yuan et al. (2007) and da Rocha et al. (2004).

2.4. Environmental driving variables

A suite of meteorological sensors measured environmental driving variables: photosynthetically active radiation (*PAR*), net radiation (*Rn*), precipitation (*Prec*), and air temperature (T_a) among others (da Rocha et al., 2009) (Supplement Table 1 and Fig. 2). Soil moisture (θ in m^3 m^{-3}) was measured using frequency-domain reflectometry (TDR) at K34 (Teixeira et al., 2003), K83 (Goulden et al., 2010) and at the control site of the Tapajos Throughfall Exclusion Experiment ($TEE_{control}$ ~ 4.5 km from the K67 tower) (Brando et al., 2006). We used consistency of relationships between similar sensors to identify and remove faulty periods and obtain a more complete meteorological time series (e.g. *Rn* and SW_{down} in W m^{-2}).

In addition to the flux and meteorological measurements, we used satellite-derived data from the Tropical Rainfall Measuring Mission (TRMM) (NASA, 2010) to obtain a consistently filled precipitation time series across all sites. We think this is justified by the observed correlation between TRMM and tower data when tower data were available (Supplement Fig. 1 and Table 2). Dry season is defined following the conventional definition for the basin, when precipitation was less than 100 mm month^{-1} (Shuttleworth, 1988).

For the estimation of reliable *PAR*, we compared *PAR* to short wave radiation (SW_{down} in W m^{-2}) data at Brasil flux network sites where both were available. At Caxiuanã (CAX), Santarém K83 and K77, Manaus (K34), and Fazenda Nossa Senora (FNS), raw *PAR* data

showed a decline over time, probably attributable to *PAR* sensor degradation, that we corrected by scaling to short wave radiation measurements, which showed no evidence of degradation. For these corrections, we derived correlation coefficients between calibrated *PAR* observations and short-wave incoming radiation measurements (*rgs* in $W\,m^{-2}$), where $PAR \sim 2 \times rgs$ (Papaioannou et al., 1993; Szeicz, 1974). *PAR* values at Pe-de-Gigante (PDG) and Bananal Island (JAV) were abnormally high. To make *PAR* ($\mu mol\,m^{-2}\,s^{-1}$) consistent to other sites we used our derived *PAR*-shortwave radiation relationship to scale *PAR* at PDG and JAV by multiplying the complete time-series by 0.79 and 0.86, respectively. *PAR* and *Rn* ($W\,m^{-2}$) were composited to 16-day intervals by simple average across all daytime and nighttime hours, as daylength (a function of time of year and latitude) is a significant driver of the variation in radiation received. Information regarding light sensors and other tower instrumentation can be found in Supplement Table 2.

We calculated hourly values of top-of-atmosphere (TOA) radiation in $W\,m^{-2}$ units, following the method of Goudriaan (1986), in which the solar constant ($1370\,J\,m^{-2}\,s^{-1}$), is modified according to orbital mechanics that can be determined by site latitude, day of year, and local time. We generated 16-day composites by simple averaging of calculated hourly values across all day and nighttime hours in each 16-day interval.

2.5. Leaf-flush model

In order to better understand the underlying processes that drive canopy scale photosynthetic assimilation, we implemented a simple model that assumes that tower-measured *Pc* ($gC\,m^{-2}\,d^{-1}$), is determined by the balance between the construction of new photosynthetic capacity (via leaf flush) and the loss of photosynthetic capacity (via litterfall):

$$\frac{dPc}{dt} = A_{max} \times SLA \times (\text{leaf flush} - \text{leaf litter fall}) \quad (1)$$

where leaf flush and litterfall quantify the mass flow of leaf matter ($gC\,m^{-2}$ ground d^{-1}) into and out of the canopy, respectively. Leaf flush and litterfall produce and remove photosynthetic capacity of the canopy according to the amount of photosynthetic capacity added or removed per unit mass of leaf, given by $A_{max} \times SLA$, the product of average leaf level photosynthetic assimilation per unit area, A_{max} ($gC\,m^{-2}$ leaf d^{-1}) and specific leaf area, *SLA* (m^2 leaf gC^{-1}). For unit conversion, we accounted carbon for 49% of the biomass (Chambers et al., 2001).

We implemented the leaf-flush model at both Santarém forest sites (K67 and K83) and at Manaus (K34), where data for litterfall (Figueira et al., 2008; Luizao and Schubart, 1987; Rice et al., 2004) and leaf-level gas exchange parameters (Carswell et al., 2000; Domingues et al., 2005) were available. *SLA* values were set to 0.0032 for K67 and K83 (Domingues et al., 2005) and to $0.0038\,m^2\,gC^{-1}$ for K34 (Carswell et al., 2000). In a first iteration, at both Tapajos forests, we assumed A_{max} to be constant and comparable to mean leaf *carbon* assimilation at saturating light (A_{max}) at 80% height, using the equation $A_{max} = 0.042 \times$ (relative height) + 5.34 (Domingues et al., 2005), $A_{max} = 8.66\,gC\,m^{-2}\,d^{-1}$ assuming most of the photosynthesis will be happening at the top of the canopy 100–80% relative height. For Manaus K34, A_{max} was set to $7.36\,gC\,m^{-2}\,d^{-1}$ following results presented by Carswell et al. (2000).

This approach likely oversimplifies canopy dynamics by assuming that the photosynthetic capacity of new and falling leaves is the same. We could improve this method by using distinct estimates of the leaf photosynthetic capacity of old and new leaves and constructing an explicit age model for the leaf pool. In the absence of more complete data, we used a sensitivity analysis where we assume that A_{max} decreases linearly starting 2 months before the peak in leaf-fall annual cycle, reaching 80%, 60% or 40% of mean A_{max}. Thus assuming that most of the abscised leaves would show a lower A_{max} and it will have an effect on the hole-ecosystem rate of assimilation.

We estimated *dPc*/*dt* by first smoothing the *Pc* time series using a LOESS (locally weighted scatter plot smoothing) regression, and then taking the derivative of a 2nd order polynomial fitted to 3 measurements (previous, target and next 16-days). Finally, we solved Eq. (1) for *leaf flush* at each 16-day time intervals.

This approach (*Pc-flush*) is similar to that employed by Doughty and Goulden (2008), who derived seasonal variations in leaf flush from variations in canopy leaf area index (*dLAI*/*dt*, estimated from light measurements above and below the canopy), except that we used the eddy flux derived quantity, *Pc*, instead of optically derived *LAI*. We compared these two approaches. For the *LAI* based approach (*LAI-flush*), we used *LAI* measurements (made with the LI-2000) on the control forest plot of the near-by drought experiment (Brando et al., 2010; Juárez et al., 2007), plugging these into a variation of Eq. (1) that replaced Pc/A_{max} with *LAI*.

2.6. Uncertainty analysis on GEP and Pc

Errors or uncertainties in characterizing the mean seasonality of photosynthetic patterns arise from at least three sources: systematic measurement bias (e.g. from failing to correctly adjust for biases arising during periods of low turbulence, Goulden et al., 1996), random sampling error, and variation in seasonality due to interannual variability in climate or other driver variables. We account for the latter two sources of uncertainty by calculating the standard deviation in measured flux in each 16-day period across the multiple years of each site's observations. However, this approach will be unlikely to account for uncertainty due to systematic measurement bias (because the same bias can persist across multiple years).

We estimated the uncertainty of measurement bias as that associated with choosing the appropriate u^*_{thresh} for filtering out periods with unrepresentatively low fluxes. We used the bootstrap method, drawing samples (with replacement) from each of the cells of the quarterly look-up table described in Section 2.2 for choosing u^*_{thresh} ($u^* - T_a - NEE$), to create 1000 bootstrap sample sets of NEE versus u^*, with each sample preserving the nighttime air temperature distribution. Each bootstrap sample gives an estimate of u^*_{thresh}. The resulting 4000 mean values (1000 samples and 4 quarters per year) are fitted to a normal distribution and the mean and 95% confidence interval of this distribution defines the uncertainty range for u^*_{thresh}, as reported in Table 1. This confidence interval in u^*_{thresh}, when propagated to results derived from *NEE* (including for *GEE*), gives an associated uncertainty range, or error, on the derived flux that arises from uncertainty in our ability to correct for the bias caused by low turbulence.

The uncertainty in correcting for bias error was added in quadrature, using a sum-of-squares approach, to the uncertainty in interannual variability (described above) to give a total uncertainty on the seasonality ($Err^2_{tot} = Err^2_{bias} + Err^2_{interannual}$). This total uncertainty is plotted as a shaded area for *GEP* and *Pc* time series in Fig. 3.

2.7. Dataset availability

All driver and flux data, as well as relevant processing codes (in Matlab) needed to reproduce this analysis are publicly available for download at http://eebweb.arizona.edu/faculty/saleska/data.htm and at http://www.climatemodeling.org/lba-mip/.

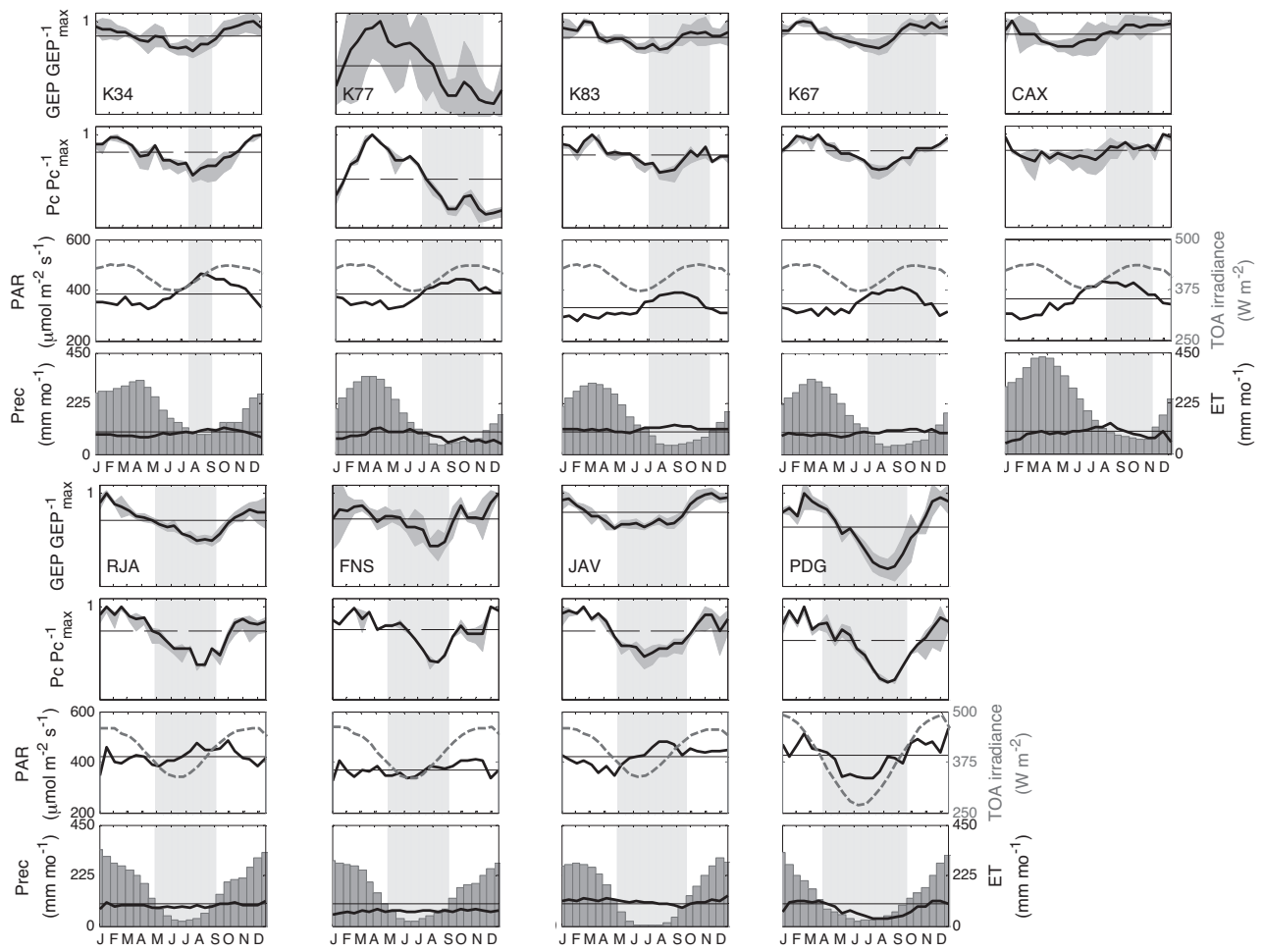

Fig. 3. Annual cycle of normalized gross ecosystem productivity, *GEP* GEP_{max}^{-1} (16-day composites) where gray uncertainty regions represent the inter-annual variability (standard deviation) of *GEP*; normalized Photosynthetic Capacity, *Pc* Pc_{max}^{-1} where gray uncertainty regions are given by the standard deviation of the 16-day *Pc* calculations ($750 > PAR < 950$). Followed by daytime photosynthetic active radiation, *PAR* (μmol m^{-2} s^{-1}) and top of the atmosphere (*TOA*) incoming solar radiation in the middle panels. At the bottom panel Precipitation, *Prec* (mm month^{-1}) based on Tropical Rainfall Measuring Mission (TRMM) data and Evapotranspiration, *ET* (mm month^{-1}). Light gray boxes indicate dry season conditions (precipitation lower than 100 mm month^{-1}). All lines represent the mean seasonal cycles, an average over all data years available for each site and the gray areas around the mean are the standard deviations when more than one year of data is available.

3. Results

3.1. Environmental conditions across Brasil flux network tower sites

Environmental and climatological conditions at the Brasil flux-sites (Supplement Table 1), show differences in seasonal patterns across the basin. Annual precipitation values (1998–2008, from TRMM) were highest at the CAX forest site (2463 mm) and lowest at the PDG savanna site (1494 mm). Precipitation at Santarém and Bananal Island forest sites (K67, K83, and JAV) is approximately 1800 mm year^{-1} and compares to rainfall at the Manaus forest (K34) and the Rondônia forest and pasture sites (RJA, FNS), both ~2000 mm year^{-1}. Dry season precipitation values, in contrast to annual values, were lower at the southern site (RJA) than at the equatorial sites. In general, dry-season length at our measurement sites is approximately five months, with CAX and K34 having the shortest dry seasons, 3 and 2 months, respectively.

The seasonality of sunlight and incoming energy at the surface arises from interacting effects of cloud cover (which reflects or absorbs radiation before reaching the surface, and peaks with precipitation), and the seasonality of incoming energy at the top-of-the atmosphere (which depends on latitude and the seasonal tilt of the earth's axis with respect to the sun). Surface *PAR* levels at equatorial Amazon sites show a seasonal cycle with a minimum in the wet season (January–March), and a maximum in the dry-season (~July to December), when reduced cloud cover increases atmospheric transmittance just as top-of-atmosphere radiation reached its second maximum with the September equinox (Fig. 3). Despite greater seasonality in top-of-atmosphere radiation at southwestern sites (RJA, FNS) 10 degrees south of the equator, there was less seasonality in surface radiation. This is a consequence of the period of minimum cloud-cover in the dry season (May–August), which is out of phase with maximum top-of-atmosphere radiation (October–February). Since dry season minimum cloud cover (maximum atmospheric transmittance) nearly coincides with minimum top-of-atmosphere radiation (June solstice), there is no obvious dry season peak in the observed surface solar radiation (Fig. 3). Moving further south to the savanna site at 22° S, the top-of-atmosphere radiation variability increases further, dominating the cloud-cover effect, so there is a strong minimum of surface *PAR* in the dry season, even though transmittance is maximized due to low cloud cover (April–October).

3.2. Seasonality of photosynthetic activity, GEP

Three distinct seasonal patterns in *GEP* were observed:

First, across the equatorial Amazon forest sites (K34, K67, K83, and CAX), *GEP* increases, or is maintained at high levels, as the dry

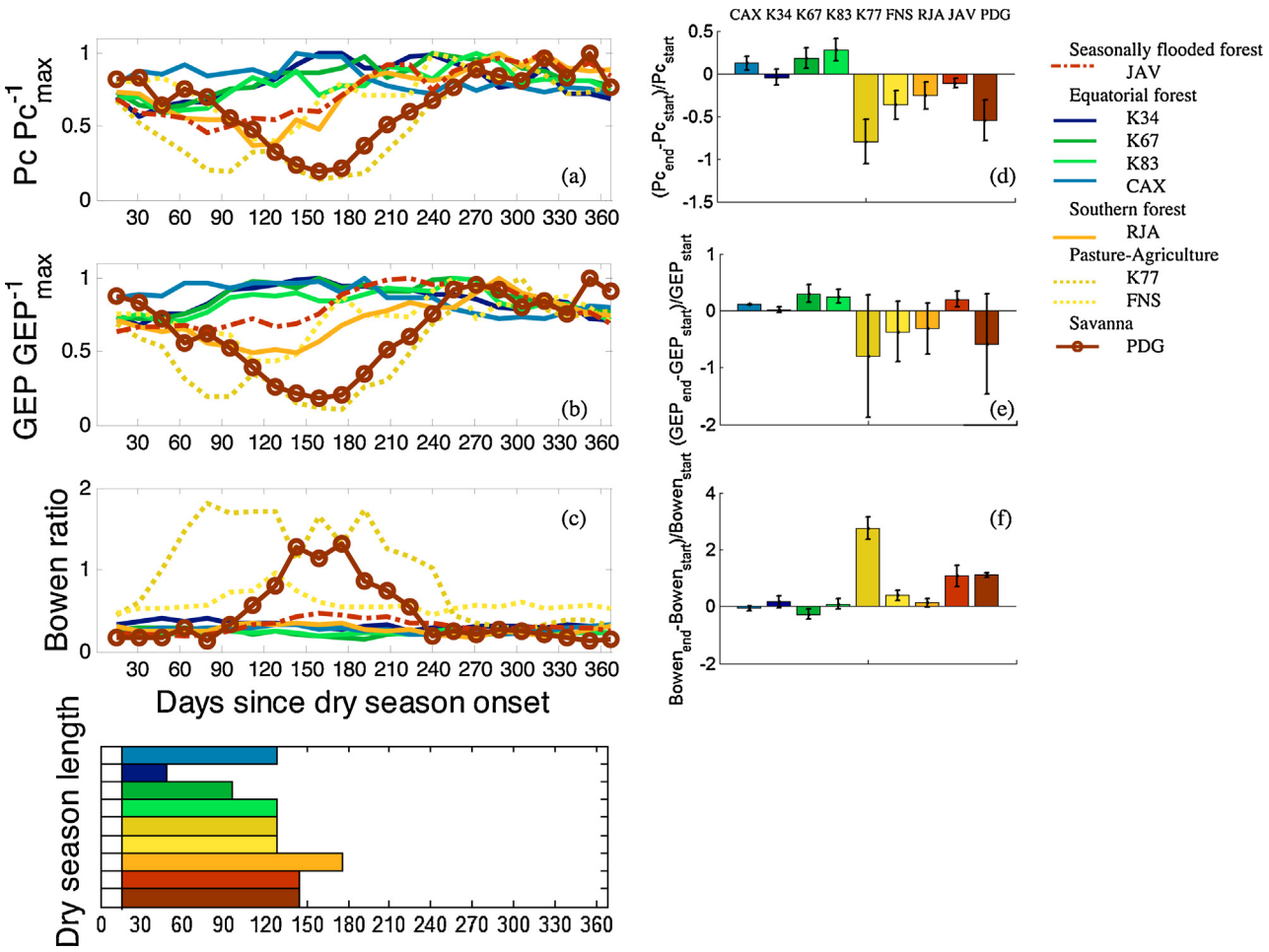

Fig. 4. Left panels (a) 16-day average normalized photosynthetic capacity, *Pc* Pc_{max}^{-1}, (b) 16-days average normalized gross ecosystem productivity, *GEP* GEP_{max}^{-1} and (c) 16-days average forest Bowen ratio (ratio between sensible heat, *LE* and sensible heat, *H*) time series set to the start of the dry season at each tower site. Right panels (d) bar plot showing the beginning-to-end of dry season change relative to the start of the season, error bars indicate site-specific interannual variability for *Pc*, (e) *GEP* and (f) Bowen ratio. Bars follow same color convention than lines.

season progresses (Figs. 3 and 4b and e). The equatorial site converted to agricultural use (K77) showed distinctly different patterns from the nearby equatorial forests, with large dry-season reductions in *GEP*, presumably a consequence of the loss of deep roots that can access deep soil water. Coinciding with the GEP decline at K77 is a sharp increase in Bowen ratio (sensible:latent heat flux ratio, Fig. 4c and f and Supplement Fig. 2), indicating significant water limitation relative to the nearby forests, which show little change in Bowen ratio.

In the second pattern, at southwestern Amazon sites (forest at RJA and pasture at FNS), *GEP* declines throughout the dry season. At these sites, the dry season tends to be more extreme than at equatorial forests and, notably, there is no distinct peak in solar radiation (Fig. 3).

An exception to the southern site pattern is the Amazon ecotone site on Bananal Island (JAV) where increasing dry-season *GEP* peaks simultaneously with *PAR* and a late dry-season decline in *ET* and increase in Bowen ratio, which remains high for the rest of the wet season (Fig. 4c and f). However, this site is seasonally flooded during the wet season, and may not experience as extreme soil dryness as the other southern sites. The seasonal wet season flooding (in February) is associated with declining *GEP*. This could be associated with anoxia, or it could be due to difficulty in interpreting eddy flux measurements during inundation. Periods of flooding are inconsistent with the standard eddy flux assumption that biosphere-atmosphere exchange captures all fluxes associated with biological activity, because significant carbon export may occur via flowing water.

The third pattern is the site in the savanna (or cerrado) biome (Fig. 3, savanna site PDG). Here, the trend from high or increasing dry season photosynthetic activity (in equatorial forests) to moderate dry season photosynthetic decline (in southern forests) reaches its extreme in the transition from forest to cerrado (Fig. 3). In comparison to forest vegetation, savanna photosynthetic metabolism exhibits a much larger range, experiencing an average reduction of 80% during the driest part of the dry season, when incoming sunlight also reaches its minimum.

3.3. Seasonality of photosynthetic capacity, Pc

Photosynthetic capacity (*Pc*) (Fig 3, second row), calculated from *GEP* within a narrow fixed range of moderately high light levels, removes the effect of differences in incoming *PAR* on productivity, giving an index of underlying photosynthetic infrastructure of the canopy (Goulden et al., 2004; Hutyra et al., 2007). *Pc* is closely related to canopy-scale Light Use Efficiency and is significantly correlated with seasonal *LAI* (Supplement Fig. 5).

The patterns of *Pc* are broadly similar to those seen for *GEP*: At equatorial Amazon sites, *Pc* either increases over the course of the dry season (CAX, K67, K83) or remains approximately constant (K34). *Pc* at these sites, like *GEP*, also remains high well into the wet

season, before declining to reach a minimum at the end of the wet season (Fig. 4a and d).

In contrast, at southern Amazon forest sites (RJA, JAV), and especially at the savanna site (PDG or at sites converted from forest (K77, FNS), *Pc* decreases as the dry season progresses and rapidly recovers after the onset of the rainfall.

We tested whether these observations of *Pc* seasonality could be an artifact of seasonal variations in *VPD* by plotting the seasonality of *Pc* defined for fixed *VPD* bins -at low (0–1 kPa), medium (1–2 kPa), and high (2–3 kPa) *VPD* levels – and comparing the results to our standard *Pc* definition across all *VPD* bins (Supplement Fig. 6). Fixed *VPD* bin *Pc* seasonalities were noisier and missing for some time-periods (because datasets constrained by both fixed light and *VPD* bins were smaller), but they showed patterns similar to those in Fig. 4: stable or increasing *Pc* at non-water limited sites (K34, K67, K83, and CAX), and *Pc* declines at the other (water-limited) sites (Supplement Fig. 6). We therefore conclude that the observed seasonal patterns of *Pc* are robust to the effect of variations in *VPD*.

3.4. Controls on seasonality of GEP and Pc

Across biomes, climates, and land uses, we observed two distinct dry season patterns (increases versus decreases in photosynthetic indices as the dry season progressed) that were largely predictable from an index of water limitation, the ratio of sensible to latent heat flux (i.e. Bowen ratio). In general, sites with access to water reserves sufficient to enable latent heat fluxes to maintain the same proportion to sensible heat fluxes in the dry season as in the wet season (Fig. 4f) also sustain or increase measures of photosynthetic capacity (Fig. 4d) or flux (Fig. 4e) in the dry season. By contrast, sites exhibiting significant increases in Bowen ratio during the dry season – whether due to land use change which removed deep roots (K77 agricultural site), natural limitation on access to deep water (RJA forest site), or absence of water during intense dry seasons (PDG savanna site) – show declines in photosynthetic capacity or flux during the same period.

However, despite access to water resources (as indicated by Bowen ratios) and high levels of dry season PAR, equatorial Amazon sites where *GEP* and *Pc* increased during the dry season showed little evidence that seasonal variation in photosynthetic activity or capacity was directly driven or limited by available energy (Fig. 4). Indeed, instead of positive correlation with *PAR*, average daytime *GEP* decreased with radiation at almost all sites across the basin, including those that exhibit dry season increases in photosynthesis (Fig. 5 top panels).

We note that this result from regression analysis is also inferable from the broad patterns observed in Sections 3.2 and 3.3, in which photosynthetic activity and capacity at equatorial sites increase throughout the dry season (when sunlight is high) but also remain high in the first part of the wet season (when sunlight is declining). These indices of photosynthesis reach their minimum at the end of the wet season, even as available sunlight is increasing.

This is in distinct contrast to controls on water fluxes: as noted in previous studies (Hasler and Avissar, 2007; da Rocha et al., 2009), *LE*, is well-correlated with net radiation (*Rn*) across most sites, even accounting for reduced sensitivity at southern forest sites (Fig. 5, second row).

Note that consistent with standard practice, we investigated *PAR* as a driver of *GEP* and net radiation as a driver of *LE*. This practice arises because photosynthetic activity is proportional to the number of photons absorbed in the 400–700 nm spectral range, and not to their energy (Alados and Alados-Arboledas, 1999), whereas evaporation is driven by total energy flux ($W\,m^{-2}$) across the solar spectrum (as captured in *Rn*). However, it is important to note that these results are robust regardless of which measure of incoming energy is used).

Despite the weak or negative association between *GEP* and radiation on average (Fig. 5), variation in PAR well-explained the deviation of *GEP* from *Pc*, when *GEP* was expressed as the fraction of photosynthetic capacity utilized: $GEP\,Pc^{-1}$ (the fraction of photosynthetic capacity, *Pc*, utilized in *GEP*) is consistently positively correlated with *PAR* at all tower sites (Fig. 6a) ($GEP = k\,PAR\,Pc$, with $k \approx 0.8–1.2\ m^2\ s\ mmol^{-1}$ for forest sites).

3.5. Leaf-flush model and analysis

GEP seasonality may be explained primarily by *Pc* seasonality, with differences between *GEP* and *Pc* explainable by light, but environmental factors do not explain *Pc* seasonality. To explore the seasonal patterns of allocation and the mechanisms that drive *Pc* we examined results from a simple leaf-flush model (Eq. (1)) at sites with sufficient data (Santarém K67 and K83, and Manaus K34). All central Amazon forests showed a peak in leaf flush during the middle of the dry season (Fig. 7). This result follows from the constraint of sustained or increasing canopy photosynthetic capacity (*Pc*) in the face of increased losses of leaf matter due to higher dry season litterfall (Rice et al., 2004).

Comparisons between a leaf-flush model driven by *Pc* (*Pc-flush*) and a *LAI* based approach (*LAI-flush*), showed that the two approaches produced consistent results at the K67 forest where we were able to compare them – there is a lag between *LAI-flush* and *Pc-flush*, which we expected, since leaves start to physically appear before their photosynthetic capacity fully develops. It takes ~10–30 days for those new leaves to reach maximum A_{max} values as reported for tropical evergreen species by Sobrado (1994). We can maximize the coefficient of determination of the relationship between the *LAI-flush* and *Pc-flush* (excluding the litterfall term), by lagging *LAI-flush* going from 0.13 (non-lagged) to 0.40 with a slope of 1.00 (32-day lag) (Supplement Fig. 3). These leaf-flush model results were also consistent with observations of *Coussarea racemosa* A. Rich (common sub-canopy tree) foliage and flower production, showing flushing-flowering coinciding with peak irradiance during the onset of the dry season (Brando et al., 2006). These comparisons indicate that leaf-flush seasonality as seen by our simplified model based in changes in ecosystem photosynthetic capacity can be used as a proxy at other sites to represent the time when the new leaves start to contribute to the CO_2 uptake.

The results from a sensitivity analysis for three leaf-flush models where A_{max} linearly decreased 2 months prior to the peak in litterfall showed a more clearly dry season peak in comparison to the leaf-flush model where we kept A_{max} constant throughout the year (Supplement Fig. 4). Thus, as decreasing ecosystem A_{max} before abscission should be counterbalance by a higher number of more productive leaves in order to maintain the observed increasing levels of Pc–a balance between quality vs. quantity of leaves.

Seasonality of leaf productivity (from the leaf-flush model) was anti-correlated with the seasonality of wood productivity during tree growth obtained from dendrometry measurements at K67 (Goulden et al., 2004; Rice et al., 2004; Saleska et al., 2003), K83 (Goulden et al., 2004) and K34 (Pereira da Silva et al., 2002). Correlation coefficients in the Tapajos (K67: $R = -0.76$, K83 $R = -0.64$, $p = 0.000$) indicate distinct differences in seasonal carbon allocation: whereas leaf production peaks in the dry season, wood production peaks in the wet season, reaching maximal values between mid-February and the end of April when soil moisture is high. This relationship was non-significant at the K34 forest near Manaus ($R = 0.1$, $p = 0.71$).

Multivariate regression models showed that leaf flush was statistically associated with sunlight, 0–40 cm volumetric soil water content ($\theta_{0–40\,cm}$), and their interaction, in a range of models (Table 2 and Supplement Table 3). Akaike's Information Criterion (AIC) selected the best models (Table 2). Because of co-linearity

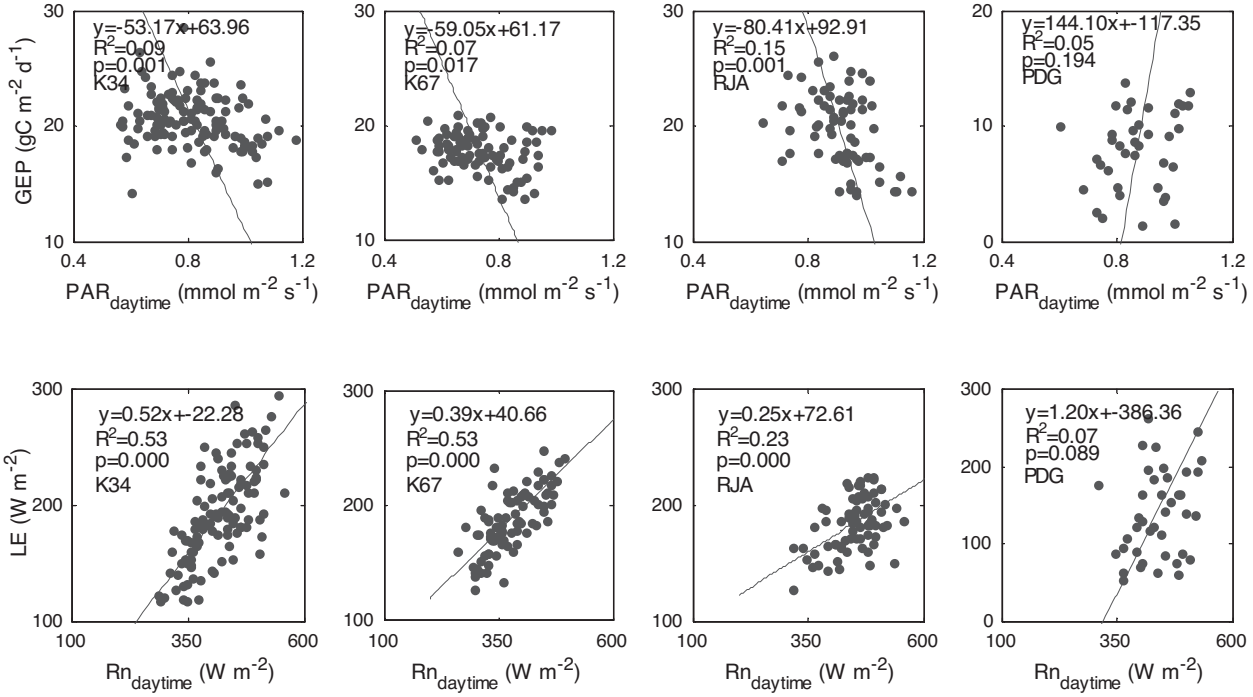

Fig. 5. Top panels: linear regression 16-day average gross ecosystem productivity, *GEP* ($gC\,m^{-2}\,d^{-1}$) versus photosynthetic active radiation, *PAR* ($mmol\,m^{-2}\,s^{-1}$). Lower panels: 16-day average latent heat flux, *LE* ($W\,m^{-2}$) versus net radiation, *Rn* ($W\,m^{-2}$) for Manaus, K34, Santarém K67 forest, Jarú, RJA and PDG savanna site.

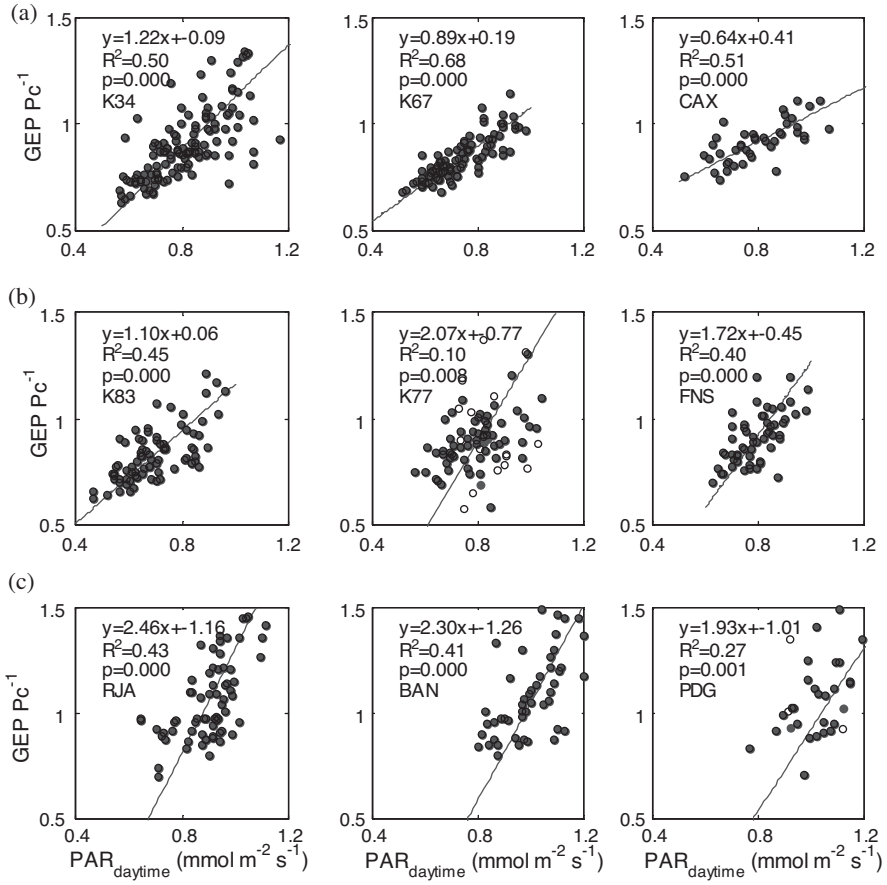

Fig. 6. Fraction of photosynthetic capacity utilized as *GEP* (dimensionless *GEP* Pc^{-1}, 16-day averages) versus photosynthetic active radiation, *PAR* ($mmol\,m^{-2}\,s^{-1}$), at: (a) Central Amazon upland forest sites (K34, K67, and CAX), (b) logged and non-forest sites (K83, K77, and FNS), where outliers (unfilled circles) corresponding to periods when ground was bare were excluded from the regression analysis for K77 (c) southern Amazon forests and cerrado sites (RJA, BAN, PDG).

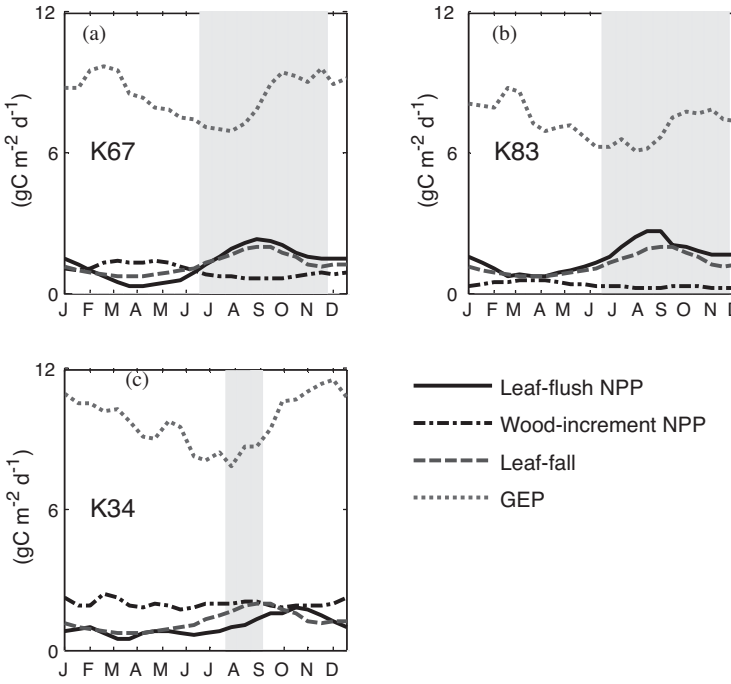

Fig. 7. Central Amazon forests (Santarém (a and b) and Manaus (c)) annual cycle of modeled leaf-flush (gC m^{-2} d^{-1}), and measurements of wood increment (gC m^{-2} d^{-1}) and gross ecosystem productivity, *GEP* (gC m^{-2} d^{-1}). Areas in gray represent precipitation < 100 mm month^{-1} based on tower and Tropical Rainfall Measuring Mission (TRMM) data.

between *PAR* (mmol m^{-2} s^{-1}) and soil moisture $\theta_{0-40\,cm}$ (e.g. at K67 $\theta_{0-40\,cm} = -0.98 \times PAR + 0.66$, R^2 of 0.21), the magnitude of coefficients should be interpreted cautiously. However, sunlight was statistically significantly positively associated with leaf flush in all models at all sites (Supplement Table 3), suggesting that this association is a robust result.

4. Discussion

Our goal is to better understand the seasonal patterns and drivers of Amazonian photosynthesis and productivity, and to provide a consistently processed database to test models of Amazon ecosystem function. Here we discuss three main questions

Table 2
Linear regressions obtained by a nonlinear mixed-effects regression model for leaf-flush (Eq. (1)) versus combinations of 16-day average *PAR* (mmol m^{-2} d^{-1}, measured at each site separately) and soil volumetric water content, (m^3 m^{-3}, measured at K83), for Santarém forest sites (K67 and K83) and Manaus (K34).

Leaf-flush	Independent variable	Coefficients		Coefficients standard error	AIC	Correlation coefficient (R^2)
K67	$[p * PAR_{daytime}\theta_{0-40\,cm}] + b$	p	10.93	−2.581	119.21	0.37
		b	−1.76	0.76		
	$[p * PAR_{daytime}(lag\,1 - month)] + b$	p	12.40	2.00	112.02	0.42
		b	−3.09	0.68		
	$[n * \theta_{0-40\,cm} * [PAR_{daytime}] + [m * \theta_{0-40\,cm}] + b$	n	32.27	5.3	45.45	0.71
		m	−19.08	0.46		
		b	3.58	2.07		
	$[n * \theta_{0-40\,cm} * [PAR_{daytime}] + [p * PAR_{daytime}] + b$	n	−23.79	4.06	44.46	0.72
		p	17.77	0.58		
		b	−2.48	1.90		
K83	$[p * PAR_{daytime}] + b$	p	9.67	1.53	94.43	0.41
		b	−1.62	0.51		
	$[p * PAR_{daytime}(lag\,1 - month)] + b$	p	9.68	1.48	93.00	0.43
		b	−1.66	0.50		
	$[n * \theta_{0-40cm} * PAR_{daytime}] + [m * \theta]_{0-40cm} + b$	n	30.56	5.18	82.18	0.53
		m	−13.49	1.66		
		b	2.55	0.46		
	$[n * \theta_{0-40\,cm} * PAR_{daytime}] + [p * PAR_{daytime}] + b$	n	−13.77	5.22	81.67	0.54
		p	12.41	1.51		
		b	−1.25	0.52		
K34	$[p * PAR_{daytime}] + b$	p	3.42	0.28	146.57	0.18
		b	−0.28	0.76		
	$[p * PAR_{daytime}(lag\,1 - month)] + b$	p	5.10	0.68	118.91	0.35
		b	−0.91	0.25		
	$[n * \theta_{0-40\,cm} * PAR_{daytime}] + [m * \theta_{0-40\,cm}] + b$	n	4.96	3.90	64.62	0.35
		m	−13.25	3.18		
		b	5.50	1.49		
	$[n * \theta_{0-40\,cm} * PAR_{daytime}] + [p * PAR_{daytime}] + b$	n	−31.05	9.99	63.67	0.35
		p	13.90	3.22		
		b	0.37	0.56		

addressed with this data: (1) What is the seasonality of photosynthesis across the Amazon basin? (2) Do environmental drivers explain observed patterns in photosynthetic seasonality? and (3) What is the role of intrinsic canopy phenology in understanding photosynthetic seasonality?

4.1. What is the seasonality of photosynthesis across the Amazon Basin?

We divided *GEP* seasonality results into three broad patterns.

The first pattern – sustained or increasing *GEP* throughout the dry season at equatorial forest sites – confirms previous individual site carbon-cycle studies near Santarem (Saleska et al., 2003; Goulden et al., 2004; Hutyra et al., 2007), and is also broadly consistent with large scale remote sensing observations of moderate dry season "green up" that used the MODIS Enhanced Vegetation Index (*EVI*) as a proxy for photosynthesis (Huete et al., 2006). These results, when combined with recent analyses showing that the dependence of forest evapotranspiration on the energy available to drive water vapor fluxes did not differ between dry and wet seasons (Costa et al., 2010b; da Rocha et al., 2004; Fisher et al., 2009; Hasler and Avissar, 2007; Hutyra et al., 2007); provide strong evidence against the idea, represented in many earlier earth-system models, that water-limitation constrains photosynthesis in equatorial Amazonian forests.

Instead, sustained or increasing dry-season *GEP* might be considered consistent with light limitation (Goulden et al., 2004; Huete et al., 2006), as these sites experience dry season peaks in irradiance, due to reduced dry-season cloud cover (see further discussion below in the section on mechanisms). This interpretation is broadly consistent with the recent generation of ecosystem modeling studies, designed to represent dry-season increases in photosynthetic metabolism (Baker et al., 2008; Kim et al., 2012).

The second pattern, observed at the southern Amazon forest site (RJA at 10° S) and the savanna biome (PDG at 20° S), is modest (RJA) or sharp (PDG) dry season declines in *GEP*. This pattern may be evidence of water stress at these sites: the southern Amazon forest (RJA) has shallower soil than the equatorial forest sites (Table 1, Kruijt et al., 2004), and may not have access to deep soil water resources, while the savanna (PDG) has climatology typical of water limited savanna biomes (with the lowest annual rainfall and driest dry season of the eddy flux sites). However, we cannot rule out simultaneous co-limitation by light, since, in contrast to the central Amazon sites, they do not experience dry season increases in light.

The contrast in photosynthesis patterns between equatorial forests and the southern forest is consistent with the analysis of water fluxes in Costa et al. (2010a), which showed that at the equatorial Amazon forests, net radiation controls *ET*, while at the southern forest (RJA) the relationship between *ET* and *Rn* was statistically less significant (Fig. 5).

A recent study based on newly available observations of chlorophyll fluorescence from the GOSAT satellite (Lee et al., 2013) concluded that regional-scale photosynthesis exhibits dry season declines in Amazon regions with moderate dry season length. This appears at odds with observations reported here for the equatorial Amazon, but consistent with those of the southern Amazon. Since Lee et al.'s (2013) findings applied only to large areas that encompassed both our equatorial and southern region towers, we cannot yet judge whether GOSAT observations are consistent with those from eddy towers.

The third pattern is associated with land-use change. The converted sites (K77, FNS) showed distinctly different seasonality from the nearby forests, with relative reductions in dry season productivity, particularly at the equatorial K77 site, where the forest pattern of dry season increases in *GEP* was completely reversed. In the southern Amazon, where the RJA forest site showed some dry season decline in photosynthesis, conversion at FNS enhanced this behavior. These dry-season reductions in *GEP* are presumably a consequence of the loss of deep roots that can access deep soil water. Simultaneous with lowered photosynthesis, dry season evapotranspiration (*ET*) is also reduced at the equatorial K77 site, apparently constrained by the low precipitation (da Rocha et al., 2004). This is in contrast to the nearby forest sites (K83 and K67) where *ET* substantially exceeds rainfall during the dry season.

Declines in photosynthesis at savanna and converted sites are likely caused by water limitation, as indicated by seasonal cycle of Bowen ratios (Fig. 4c and f). The ratio shows that relative to the approximately constant sensible to latent heat flux ratio in forests (Supplement Fig. 2), conversion or shift in biome from forest to savanna causes energy fluxes to the atmosphere to be carried much more by sensible heat, as water supply to drive the latent heat flux is sharply reduced.

In sum, differences in seasonal *GEP* patterns appear closely associated with difference in climatology, biome type, and land use (Fig. 3). Along a North-South climate gradient, differences in *GEP* patterns correspond to declines in precipitation and/or shifts in the seasonality of irradiance. Near the equator irradiance peaks in the relatively cloud-free dry season; in the southern Amazon there is no seasonality (dry-season minimum in top-of-atmosphere irradiance nullifies the effect of reduced cloud cover); and at the high-latitude southern savanna, strong seasonality gives a dry-season *minimum* in irradiance (opposite in phase to the equatorial sites).

Next, we discuss specific tests for whether annual cycle in environmental variables is associated with photosynthesis patterns.

4.2. Do environmental drivers explain observed patterns in photosynthetic seasonality?

How are equatorial Amazon forests able to sustain high levels of photosynthetic capacity, even throughout dry seasons that many of the early model studies suggested should lead to water-limited reductions in photosynthesis?

Observations of exceptionally deep tree roots (up to 18 m) (Hodnett et al., 1996; Nepstad et al., 1994), of hydraulic redistribution by roots (da Rocha et al., 2004; Oliveira et al., 2005), and of seasonal shifts in the water supply for *ET* from shallow (3 m) to deep (>7 m) soil layers between wet and dry seasons (Bruno et al., 2006) suggest mechanisms by which water limitation may be circumvented. These mechanism, could allow tropical forests to maintain access to non-transient stores of deep soil water, even when the surface becomes sufficiently dry to limit biological activity. Such mechanisms were missing from early models, as many were built around more studied temperate and agricultural systems, and which typically represent forests as having 2–3 m rooting depths.

If the deep-soil water hypothesis explains the maintenance of dry season photosynthesis, this predicts that removing access to deep soil water should reverse dry season *GEP* patterns. This is precisely what is observed with conversion of equatorial forest (e.g. K77, Fig. 4), which induces the effect of the forest-savanna transition by converting forest from a dry season "green-up" to a "brown-down" pattern, presumably due to the removal of deep roots, which allow for access to stored water during dry periods.

Thus, this study confirms earlier suggestions that many Amazon forests have mechanisms that allow them to escape water limitation. However, a new result of this study is the general finding that, across both sites that are water limited and those that are not, photosynthesis also shows no simple relation to sunlight (Fig. 5). At all Amazonian sites bi-weekly *GEP* shows a weak or declining relation with increasing light, contradicting assumptions of many models that days with high light are consistently more productive than days with low light. Only at the savanna site (PDG) was there

a (weakly) positive relation between 16-day average *GEP* and *PAR* (Fig. 5 far right panel).

These patterns imply that combined canopy-scale evaporation and transpiration (i.e. total latent energy flux, tightly correlated with available energy) are decoupled from photosynthesis (which is uncorrelated or negatively correlated with available energy) (Fig. 5). If plant transpiration is coupled to photosynthesis, as is usually assumed, this suggests that the contribution of non-plant regulated evaporation must vary in tandem with photosynthetically coupled transpiration to maintain whole-ecosystem water flux that remains correlated with incoming energy.

We considered whether the lack of correlation between *GEP* and sunlight, and the divergence of this observation with *LE* response to incoming energy, was a consequence of photosynthetic saturation with respect to PAR, at least in the dry season. However, the available evidence suggests it is not. In particular, because sunlight still drives fluctuations in GEP relative to photosynthetic capacity (Fig. 6), it is unlikely that GEP is saturated. A more likely explanation, is simply that the underlying canopy photosynthetic capacity, a dominant control on photosynthetic flux, follows a seasonality determined by endogenous biological seasonal cycles of litterfall and leaf flush, and these are only indirectly related to sunlight (see Section 4.3, below).

In sum, canopy photosynthesis (in contrast to *ET*) cannot be modeled as a simple increasing function of available energy or sunlight. Consequently, observed patterns of photosynthesis and potential driving variables are not only inconsistent with ecosystem models that assume water limitation in these forests (Lee et al., 2005; Nobre et al., 1991; Werth and Avissar, 2002), but also with non-water limited light use efficiency models that are based on the assumption of constant photosynthetic capacity interacting with varying light levels (Xiao et al., 2005).

4.3. What is the role of intrinsic canopy phenology in understanding photosynthetic seasonality?

Taken together, the analysis presented here suggests that there is significant seasonal variation in standing canopy photosynthetic capacity (*Pc*, second row, Fig. 3), even in these evergreen forests. In other words, we find that canopy phenology, not environmental variability, is the dominant control on the seasonality of tropical forest photosynthesis, across all studied regions. The dominant seasonality of photosynthetic flux (*GEP*) simply follows that of the seasonality of the canopy photosynthetic capacity. *GEP* deviations from the primary pattern set by *Pc* are explained by variations in sunlight availability, which effectively regulates the fraction of photosynthetic capacity utilized (*GEP*/*Pc*) (Fig. 6). This suggests that if canopy photosynthetic capacity were constant (as many ecosystem models assume for tropical evergreen forests), then the seasonality of GEP at non water-limited sites would indeed be well-explained by the seasonality of sunlight.

For example, a recent study of Amazon forest photosynthetic seasonality using the new method of satellite-observed fluorescence (Lee et al., 2013) assumed that *LAI* was constant, leading them to conclude that "*GPP* changes are more related to environmental conditions" than to changes in canopy photosynthetic infrastructure, a conclusion not supported by the tower-derived observations reported here.

As noted by Doughty and Goulden (2008) based on observations at the K83 site alone, this seasonal variation in canopy photosynthetic capacity poses a challenge for modeling efforts. Though many ecosystem models allow *Pc* to be specified exogenously, e.g. as varying *LAI* (BIOME-BGC (Thornton et al., 2002), LPJ (Sitch et al., 2003), CASA (Potter, 2003), Orchidee (Krinner et al., 2005) and other Land Surface Models), few are able to prognostically simulate variation in photosynthetic infrastructure in evergreen tropical forests (for a simple recent approach to this problem, however, see Kim et al., 2012).

This raises the question: what controls the seasonal variation in canopy photosynthetic capacity? and in particular, why is it not well correlated with sunlight? Here, we used a simple the leaf flush model to characterize the underlying process that give rise to canopy photosynthetic capacity, and investigate their relation to environmental drivers.

The leaf flush model embodies the constraint that changes in canopy photosynthetic capacity must arise from the difference between the creation of new capacity (leaf flush) and the loss of existing capacity (leaf abscission and litterfall). Leaf flush and litterfall likely arise from evolutionary strategies that are mostly beyond the scope of this study, but we can hypothesize here about which strategies might be adaptive in which climates. Litterfall at the three equatorial Amazon sites peaks in the dry season (Rice et al., 2004; Figueira et al., 2008). Though the seasonal cycle of leaf abscission has been interpreted as implying that *LAI* and productivity should decline in the dry season, our observations of simultaneously increasing dry-season photosynthetic capacity at these sites requires a dry-season peak in leaf flush sufficient to more than compensate for the peak in litterfall (Fig. 7). This dry season peak in leaf flush, together with multiple regression analysis (Table 2 and Supplement Table 3) showing consistent positive correlation, across sites and regression models, between leaf flush and light, suggests that leaf growth is light limited.

High dry-season light levels drive new leaf production in the dry season, which in turn drives increases in *Pc* and *GEP* that should level off, or maximize, only when leaf production declines to zero, at the end of the dry season; this expected late dry-season peak in *GEP*, lagging that of leaf flush, is especially visible at the Tapajos sites (Fig. 7).

The leaf flush model thus helps explain features of the observed seasonal patterns of photosynthesis and light. If leaf growth (not photosynthetic capacity directly) is light limited, then the higher photosynthetic capacity that follows from high dry season leaf production should lag leaf growth, and persist into the wet season, also driving high *GEP* during the dry-wet season transition. This pushes *GEP* out of phase with sunlight, explaining the negative observed relationship between *GEP* and incoming radiation.

We hypothesize that seasonality in tropical forest *Pc* arises when limiting resources for leaf growth are seasonal. This hypothesis is supported by observations in this study and in the literature. For example, if the growth of leaves is light-limited, production of new leaves should occur during the season of maximal irradiance (a pattern typically seen in studies of tropical vegetation phenology, e.g. Borchert, 1980; Wright and Van Schaik, 1994), and equatorial climates with high dry-season light levels should benefit vegetation that grows leaves in the dry season (as seen in Fig. 7).

This benefit should also control allocation patterns within individuals, such that during high-irradiance periods, allocation to leaf production should be prioritized over allocation to growth of other organs. Just such a seasonal cycle in allocation patterns can be seen between leaf flush and wood growth (Fig. 7) in some of our equatorial sites, where production of leaves (which grow in the dry season) is out-of-phase with that of wood (which grows in the wet season). This pattern could be altered when other resource constraints become more pressing than that of light. For example, in seasonally inundated floodplain tropical forests, where anoxia limits respiratory requirements of wood growth during wet seasons, wood growth phenology should also be shifted into the dry season, as has been observed in tree-ring records from seasonally flooded Amazon forests (Dezzeo et al., 2003).

By contrast, in climates with no strong seasonality in irradiance (as at the southern forest site, RJA), light-based growth strategies would not be advantageous, and seasonal patterns would not favor

dry season leaf production. There is only one southern upland Amazonian forest site (RJA), and we do not have long-term litterfall data from this site, so our ability to test this hypothesis for southern sites is limited. However, the dry season declines in Pc observed here would be consistent with absence of dry season leaf growth following from no increase in dry season irradiance at this site.

Stronger conclusions about whether southern forests are truly water limited (e.g. due to relatively shallower soils as in von Randow et al., 2004), or simply experience little or no resource benefit from elevated dry season metabolism, would require more observations in this region of the Amazon.

5. Conclusions

Integrated study across Amazonian eddy flux towers provide new insights into the drivers on the seasonality of photosynthetic metabolism in tropical systems, the different factors which influence metabolism in different biomes and climate zones, and the ways in which human changes to the landscape alter ecosystem functions along with the changes in structure.

First, although southerly Amazon forests, strongly seasonal savanna, and sites converted from forest to agricultural uses exhibit photosynthetic and energy flux patterns consistent with water-limitation, other sites do not. In particular, high or increasing levels of photosynthetic activity observed during the dry season in equatorial forests, together with no water limitation observed in the seasonality of the ratio of sensible to latent heat flux (the Bowen ratio), provide strong evidence against the common idea that water-limitation constrains photosynthesis in these forests.

Second, even though our analysis suggests that the seasonality of photosynthesis in equatorial Amazonian forests is not water limited, nor is it limited by sunlight in a simple way. Rather, photosynthetic fluxes largely follow the biologically determined phenology of canopy photosynthetic capacity, which itself is driven by patterns of leaf flush and litterfall. Light can affect canopy photosynthetic capacity indirectly, and with time lags, by driving leaf growth.

Third, equatorial climates benefit vegetation that can grow leaves in the dry season, when surface solar radiation peaks. By contrast, southerly forests may not allocate to new leaves to increase their photosynthetic activity and capacity in the dry season, either because water limitation prevents them, or because lack of seasonality in surface radiation implies that no benefits accrue from such strategies.

This analysis of the seasonality of photosynthetic metabolism provides a window onto the mechanisms controlling photosynthetic metabolism of Amazon vegetation, showing that responses to seasonal climate variation are complex, and pose challenges to models seeking to represent Amazon forest responses to climatic variation.

Acknowledgments

Author contributions. First author NRC and senior author SRS designed the research. NRC conducted the research with contributions from SRS and HRdR. NRC and SRS wrote the paper, with significant contributions from HRdR, LRH, ACdA, BC, DRF, MLG, BK, and SCW. Key datasets, interpretations thereof, and editorial comments on the text were contributed by all remaining authors. This research was funded by the National Aeronautics and Space Administration (NASA) (LBA investigation CD-32 and the LBA-DMIP project, award #NNX09AL52G), the National Science Foundation (Amazon-PIRE, NSF award #OISE-0730305), and the Gordon and Betty Moore Foundation's Andes-Amazon Initiative. Second author acknowledges Fapesp (02/09289-9) and CNPq (Instituto do Milênio–LBA, Ed. Universal-01, Ed. CT-Hidro 03). The authors would like to thank Dr. Joost van Haren, Dr. Alfredo Huete, Dr. Piyachat Ratana and the staff of each tower site for their technical, logistical and extensive fieldwork. Finally, the authors are also extremely grateful to four reviewers that with their comments improved the initial manuscript.

Appendix A. Supplementary data

Supplementary data associated with this article can be found, in the online version, at http://dx.doi.org/10.1016/j.agrformet.2013.04.031.

References

Alados, I., Alados-Arboledas, L., 1999. Direct and diffuse photosynthetically active radiation: measurements and modelling. Agricultural and Forest Meteorology 93, 27–38.

Andreae, M.O., Artaxo, P., Brandão, C., Carswell, F.E., Ciccioli, P., da Costa, A.L., Culf, A.D., Esteves, J.L., Gash, J.H.C., Grace, J., Kabat, P., Lelieveld, J., Malhi, Y., Manzi, A.O., Meixner, F.X., Nobre, A.D., Nobre, C., Ruivo, M.d., Silva-Dias, L.P., Stefani, M.A., Valentini, P., Jouanne, R., von, J., Waterloo, M.J., 2002. Biogeochemical cycling of carbon, water, energy, trace gases, and aerosols in Amazonia: the LBA-EUSTACH experiments. J. Geophys. Res. 107, 25.

Araújo, A.C., Nobre, A.D., Kruijt, B., Elbers, J.A., Dallarosa, R., Stefani, P., Randow, C., von Manzi, A.O., Culf, A.D., Gash, J.H.C., Valentini, R., Kabat, P., 2002a. Comparative measurements of carbon dioxide fluxes from two nearby towers in a central Amazonian rainforest: the Manaus LBA site. J. Geophys. Res. 107, 8090.

Araújo, A.C., Nobre, A.D., Kruijt, B., Elbers, J.A., Dallarosa, R., Stefani, P., Randow, C., von Manzi, A.O., Culf, A.D., Gash, J.H.C., Valentini, R., Kabat, P., 2002b. Comparative measurements of carbon dioxide fluxes from two nearby towers in a central Amazonian rainforest: the Manaus LBA site. J. Geophys. Res. 107, 20.

Aubinet, M., 2008. Eddy covariance CO_2 flux measurements in nocturnal conditions: an analysis of the problem. Ecol. Appl. 18, 1368–1378.

Baker, I.T., Prihodko, L., Denning, A.S., Goulden, M., Miller, S., da Rocha, H.R., 2008. Seasonal drought stress in the Amazon: reconciling models and observations. J. Geophys. Res. 113, G00B01.

Barr, A., Hollinger, D.Y., Richardson, A.D., 2009. NACP Uncertainty Analysis.

Betts, R.A., Cox, P.M., Collins, M., Harris, P.P., Huntingford, C., Jones, C.D., 2004. The role of ecosystem–atmosphere interactions in simulated Amazonian precipitation decrease and forest dieback under global climate warming. Theor. Appl. Climatol. 78, 157–175.

Borchert, R., 1980. Phenology and ecophysiology of tropical trees: *Erythrina poeppigiana* O.F. Cook. Ecology 61, 1065–1074.

Borma, L.S., da Rocha, H.R., Cabral, O.M., von Randow, C., Collicchio, E., Kurzatkowski, D., Brugger, P.J., Freitas, H., Tannus, R., Oliveira, L., Rennó, C.D., Artaxo, P., 2009. Atmosphere and hydrological controls of the evapotranspiration over a floodplain forest in the Bananal Island region, Amazonia. J. Geophys. Res. 114, 12.

Botta, A., Ramankutty, N., Foley, J.A., 2002. Long-term variations of climate and carbon fluxes over the Amazon basin. Geophys. Res. Lett. 29, 4.

Brando, P., Ray, D., Nepstad, D., Cardinot, G., Curran, L.M., Oliveira, R., 2006. Effects of partial throughfall exclusion on the phenology of *Coussarea racemosa* (Rubiaceae) in an east-central Amazon rainforest. Oecologia 150, 181–189.

Brando, P.M., Goetz, S.J., Baccini, A., Nepstad, D.C., Beck, P.S.A., Christman, M.C., 2010. Seasonal and interannual variability of climate and vegetation indices across the Amazon. Proc. Natl. Acad. Sci. USA 107, 14685–14690.

Bruno, R.D., Rocha, H.R.da, de Freitas, H.C., Goulden, M.L., Miller, S.D., 2006. Soil moisture dynamics in an eastern Amazonian tropical forest. Hydrol. Processes 20, 2477–2489.

Carswell, F.E., Costa, A.L., Palheta, M., Malhi, Y., Meir, P., Costa, J.de.P.R., Ruivo, M.de.L., Leal, L.do.S.M., Costa, J.M.N., Clement, R.J., Grace, J., 2002. Seasonality in CO_2 and H_2O flux at an eastern Amazonian rain forest. J. Geophys. Res. 107, 16.

Carswell, F.E., Meir, P., Wandelli, E.V., Bonates, L.C.M., Kruijt, B., Barbosa, E.M., Nobre, A.D., Grace, J., Jarvis, P.G., 2000. Photosynthetic capacity in a central Amazonian rain forest. Tree Physiol. 20, 179–186.

Chambers, J.Q., Dos Santos, J., Ribeiro, R., Higuchi, N., 2001. Tree damage, allometric relationships, and aboveground net primary production in a tropical forest. For. Ecol. Manage. 152, 73–84.

Costa, M.H., Biajoli, M.C., Sanches, L., Malhado, A.C.M., Hutyra, L.R., da Rocha, H.R., Aguiar, R.G., de Araújo, A.C., 2010a. Atmospheric versus vegetation controls of Amazonian tropical rain forest evapotranspiration: are the wet and seasonally dry rain forests any different? J. Geophys. Res. 115, 9.

Costa, M.H., Biajoli, M.C., Sanches, L., Malhado, A.C.M., Hutyra, L.R., da Rocha, H.R., Aguiar, R.G., de Araújo, A.C., 2010b. Atmospheric versus vegetation controls of Amazonian tropical rain forest evapotranspiration: are the wet and seasonally dry rain forests any different? J. Geophys. Res. 115, G04021.

da Rocha, H.R., Freitas, H.C., Rosolem, R., Juarez, R.I.N., Tannus, R., Ligo, M.A., Cabral, O.M., Silva-Dias, M.A.F., 2002. Measurements of CO exchange over a woodland savanna (Cerrado sensu stricto) in southeast Brasil. Biota Neotropica 2, BN01702012002.

da Rocha, H.R., Goulden, M.L., Miller, S.D., Menton, M.C., Pinto, L.D.V.O., De Freitas, H.C., E Silva Figueira, A.M., 2004. Seasonality of water and heat fluxes over a tropical forest in Eastern Amazonia. Ecol. Appl. 14, 22–32.

da Rocha, H.R., Manzi, A.O., Cabral, O.M., Miller, S.D., Goulden, M.L., Saleska, S.R., Restrepo-Coupe, N., Wofsy, S.C., Borma, L.S., Artaxo, P., Vourlitis, G., Nogueira, J.S., Cardoso, F.L., Nobre, A.D., Kruijt, B., Freitas, H.C., von Randow, C., Aguiar, R.G., Maia, J.F., 2009. Patterns of water and heat flux across a biome gradient from tropical forest to savanna in Brazil. J. Geophys. Res. 114, 8.

Dezzeo, N., Worbes, M., Ishii, I., Herrera, R., 2003. Annual tree rings revealed by radiocarbon dating in seasonally flooded forest of the Mapire River, a tributary of the lower Orinoco River, Venezuela. Plant Ecol. 168, 165–175.

Dickinson, R.E., Henderson-Sellers, A., 1988. Modelling tropical deforestation: a study of GCM land-surface parametrizations. Quart. J. R. Meteorol. Soc. 114, 439–462.

Domingues, T.F., Berry, J.A., Martinelli, L.A., Ometto, J.P.H.B., Ehleringer, J.R., 2005. Parameterization of canopy structure and leaf-level gas exchange for an Eastern Amazonian tropical rain forest (Tapajós National Forest, Pará, Brazil). Earth Interact. 9, 1.

Doughty, C.E., Goulden, M.L., 2008. Seasonal patterns of tropical forest leaf area index and CO_2 exchange. J. Geophys. Res. 113, 12.

Fidelis, A.T., de Godoy, S.A.P., 2003. Estrutura de um cerrado strico sensu na Gleba Cerrado Pé-de-Gigante, Santa Rita do Passa Quatro SP. Acta Bot. Brasil. 17, 531–539.

Figueira, A.M.eS., Miller, S.D., Sousa, C.A.D.de, Menton, M.C., Maia, A.R., da Rocha, H.R., Goulden, M.L., 2008. Effects of selective logging on tropical forest tree growth. J. Geophys. Res. 113, 11.

Fisher, J.B., Malhi, Y., Bonal, D., da Rocha, H.R., De AraâšJo, A.C., Gamo, M., Goulden, M.L., Hirano, T., Huete, A.R., Kondo, H., Kumagai, T., Loescher, H.W., Miller, S., Nobre, A.D., Nouvellon, Y., Oberbauer, S.F., Panuthai, S., Roupsard, O., Saleska, S., Tanaka, K., Tanaka, N., Tu, K.P., von Randow, C., 2009. The landâ "atmosphere water flux in the tropics". Global Change Biol. 15, 2694–2714.

Friedlingstein, P., Cox, P., Betts, R., Bopp, L., Von Bloh, W., Brovkin, V., Cadule, P., Doney, S., Eby, M., Fung, I., Bala, G., John, J., Jones, C., Joos, F., Kato, T., Kawamiya, M., Knorr, W., Lindsay, K., Matthews, H.D., Raddatz, T., Rayner, P., Reick, C., Roeckner, E., Schnitzler, K.-G., Schnur, R., Strassmann, K., Weaver, A.J., Yoshikawa, C., Zeng, N., 2006. Climate–carbon cycle feedback analysis: results from the C4MIP model intercomparison. J. Climate 19, 3337–3353.

Frankenberg, C., Fisher, J.B., Worden, J., Badgley, G., Saatchi, S.S., Lee, J.-E., Toon, G.C., Butz, A., Jung, M., Kuze, A., Yokota, T., 2011. New global observations of the terrestrial carbon cycle from GOSAT: Patterns of plant fluorescence with gross primary productivity. Geophysical Research Letters 38.

Goudriaan, J., 1986. A simple and fast numerical method for the computation of daily totals of crop photosynthesis. Agric. For. Meteorol. 38, 249–254.

Goulden, M.L., Miller, S.D., da Rocha, H.R., Menton, M.C., De Freitas, H.C., E Silva Figueira, A.M., De Sousa, C.A.D., 2004. Diel and seasonal patterns of tropical forest CO_2 exchange. Ecol. Appl. 14, 42–54.

Goulden, M.L., Miller, S.D., da Rocha, H.R., 2010. LBA-ECO CD-04 Soil Moisture Data, km 83 Tower Site, Tapajos National Forest, Brazil. Data set. Oak Ridge National Laboratory Distributed Active Archive Center http://daac.ornl.gov

Goulden, M.L., Munger, J.W., Fan, S.-M., Daube, B.C., Wofsy, S.C., 1996. Measurements of carbon sequestration by long-term eddy covariance: methods and a critical evaluation of accuracy. Global Change Biol. 2, 169–182.

Gu, L., Fuentes, J.D., Garstang, M., da Silva, J.T., Heitz, R., Sigler, J., Shugart, H.H., 2001. Cloud modulation of surface solar irradiance at a pasture site in southern Brazil. Agric. For. Meteorol. 106, 117–129.

Hasler, N., Avissar, R., 2007. What controls evapotranspiration in the Amazon Basin? J. Hydrometeorol. 8, 380–395.

Hodnett, M.G., Oyama, M.D., Tomasella, J., Marques, A.de.O.F., 1996. Comparisons of long-term soil water storage behavior under pasture and forest in three areas of Amazonia. In: Amazonia Deforestation and Climate. John Wiley, New York, USA, pp. 57–77.

Horel, J.D., Hahmann, A.N., Geisler, J.E., 1989. An investigation of the annual cycle of convective activity over the Tropical Americas. J. Climate 2, 1388–1403.

Huete, A.R., Didan, K., Shimabukuro, Y.E., Ratana, P., Saleska, S.R., Hutyra, L.R., Yang, W., Nemani, R.R., Myneni, R., 2006. Amazon rainforests green-up with sunlight in dry season. Geophys. Res. Lett. 33, 4.

Hutyra, L.R., Munger, J.W., Saleska, S.R., Gottlieb, E., Daube, B.C., Dunn, A.L., Amaral, D.F., De Camargo, P.B., Wofsy, S.C., 2007. Seasonal controls on the exchange of carbon and water in an Amazonian rain forest. J. Geophys. Res. 112.

Hutyra, L.R., Munger, J.W., Hammond-Pyle, E., Saleska, S.R., Restrepo-Coupe, N., Daube, B.C., de Camargo, P.B., Wofsy, S.C., 2008. Resolving systematic errors in estimates of net ecosystem exchange of CO_2 and ecosystem respiration in a tropical forest biome. Agricultural and Forest Meteorology 148, 1266–1279.

Iwata, H., Malhi, Y., von Randow, C., 2005. Gap-filling measurements of carbon dioxide storage in tropical rainforest canopy airspace. Agricultural and Forest Meteorology 132, 305–314.

Juárez, R.I.N., Hodnett, M.G., Fu, R., Goulden, M.L., von Randow, C., 2007. Control of dry season evapotranspiration over the Amazonian forest as inferred from observations at a Southern Amazon forest site. J. Climate 20, 2827–2839.

Jurik, T.W., 1986. Seasonal patterns of leaf photosynthetic capacity in successional northern Hardwood tree species. Am. J. Bot. 73, 131–138.

Keller, M., Alencar, A., Asner, G.P., Braswell, B., Bustamante, M., Davidson, E., Feldpausch, T., Fernandes, E., Goulden, M., Kabat, P., Kruijt, B., Luizão, F., Miller, S., Markewitz, D., Nobre, A.D., Nobre, C.A., Filho, N.P., da Rocha, H., Dias, P.S., von Randow, C., Vourlitis, G.L., 2004. Ecological research in the large-scale biosphere–atmosphere experiment in Amazonia: early results. Ecol. Appl. 14, S3–S16.

Kim, Y., Knox, R.G., Longo, M., Medvigy, D., Hutyra, L.R., Pyle, E.H., Wofsy, S.C., Bras, R.L., Moorcroft, P.R., 2012. Seasonal carbon dynamics and water fluxes in an Amazon rainforest. Global Change Biol. 18, 1322–1334.

Koren, I., Kaufman, Y.J., Remer, L.A., Martins, J.V., 2004. Measurement of the effect of Amazon smoke on inhibition of cloud formation. Science 303, 1342–1345.

Krinner, G., Viovy, N., de Noblet-Ducoudré, N., Ogée, J., Polcher, J., Friedlingstein, P., Ciais, P., Sitch, S., Prentice, I.C., 2005. A dynamic global vegetation model for studies of the coupled atmosphere-biosphere system. Global Biogeochemical Cycles 19.

Lasslop, G., Reichstein, M., Papale, D., Richardson, A.D., Arneth, A., Barr, A., Stoy, P., Wohlfahrt, G., 2010. Separation of net ecosystem exchange into assimilation and respiration using a light response curve approach: critical issues and global evaluation. Global Change Biology 16, 187–208.

Lloyd, J., Farquhar, G.D., 2008. Effects of rising temperatures and [CO_2] on the physiology of tropical forest trees. Philos Trans R SocLond B BiolSci 363, 1811–1817.

Kruijt, B., Elbers, J.A., von Randow, C., Araújo, A.C., Oliveira, P.J., Culf, A., Manzi, A.O., Nobre, A.D., Kabat, P., Moors, E.J., 2004. The robustness of eddy correlation fluxes for Amazon rain forest conditions. Ecol. Appl. 14, 101–113.

Lee, J.-E., Oliveira, R.S., Dawson, T.E., Fung, I., 2005. Root functioning modifies seasonal climate. Proc. Natl. Acad. Sci. USA 102, 17576–17581.

Lee, J.-E., Frankenberg, C., Tol, C., van der, Berry, J.A., Guanter, L., Boyce, C.K., Fisher, J.B., Morrow, E., Worden, J.R., Asefi, S., Badgley, G., Saatchi, S., 2013. Forest productivity and water stress in Amazonia: observations from GOSAT chlorophyll fluorescence. Proc. R. Soc. B 280.

Luizao, F.J., Schubart, H.O.R., 1987. Litter production and decomposition in a terra-firme forest of central Amazonia. Experientia 43, 259–265.

Malhi, Y., Aragao, L.E.O.C., Metcalfe, D.B., Paiva, R., Quesadas, C.A., Almeida, S., Anderson, L., Brando, P., Chambers, J.Q., Da Costa, A.C.L., Hutyra, L.R., Olivera, P., Patino, S., Pyle, E.H., Robertson, A.L., Texteira, L.M., 2009. Comprehensive assessment of carbon productivity, allocation and storage in three Amazonian forests. Global Change Biol., http://dx.doi.org/10.1111/j.1365-2486.2008.01780.x.

Malhi, Y., Nobre, A.D., Grace, J., Kruijt, B., Pereira, M.G.P., Culf, A., Scott, S., 1998. Carbon dioxide transfer over a Central Amazonian rain forest. J. Geophys. Res. 103, 31593–31612.

Malhi, Y., Pegoraro, E., Nobre, A.D., Pereira, M.G.P., Grace, J., Culf, A.D., Clement, R., 2002. Energy and water dynamics of a central Amazonian rain forest. J. Geophys. Res. 107, LBA 45–1–LBA 45–17.

Miller, S.D., Goulden, M.L., Menton, M.C., da Rocha, H.R., de Freitas, H.C., E Silva Figueira, A.M., de Sousa, C.A.D., 2004. Biometric and micrometeorological measurements of tropical forest carbon balance. Ecol. Appl. 14, S114–S126.

Monteith, J.L., 1965. Evaporation and environment. In: The State and Movement of Water in Living Organisms. Cambridge University Press, Swansea/Cambridge, UK, pp. 205–234.

Myneni, R.B., Yang, W., Nemani, R.R., Huete, A.R., Dickinson, R.E., Knyazikhin, Y., Didan, K., Fu, R., Negrón Juárez, R.I., Saatchi, S.S., Hashimoto, H., Ichii, K., Shabanov, N.V., Tan, B., Ratana, P., Privette, J.L., Morisette, J.T., Vermote, E.F., Roy, D.P., Wolfe, R.E., Friedl, M.A., Running, S.W., Votava, P., El-Saleous, N., Devadiga, S., Su, Y., Salomonson, V.V., 2007. Large seasonal swings in leaf area of Amazon rainforests. Proc. Natl. Acad. Sci. 104, 4820–4823.

NASA, 2010. Tropical Rainfall Measuring Mission (TRMM) (1998–2006 mean), Monthly 0.25 0.25 TRMM and Other Sources Rainfall. NASA Distrib. Active Arch. Cent., Goddard Space Flight Cent. Earth Sci., Greenbelt, MD (accessed 27.07.10) http://mirador.gsfc.nasa.gov/cgi-bin/mirador/

Negrón Juárez, R.I., da Rocha, H.R., E Figueira, A.M.S., Goulden, M.L., Miller, S.D., 2009. An improved estimate of leaf area index based on the histogram analysis of hemispherical photographs. Agric. For. Meteorol. 149, 920–928.

Nepstad, D.C., De Carvalho, C.R., Davidson, E.A., Jipp, P.H., Lefebvre, P.A., Negreiros, G.H., Da Silva, E.D., Stone, T.A., Trumbore, S.E., Vieira, S., 1994. The role of deep roots in the hydrological and carbon cycles of Amazonian forests and pastures. Nature 372, 666–669.

Nepstad, D.C., Moutinho, P., Dias-Filho, M.B., Davidson, E., Cardinot, G., Markewitz, D., Figueiredo, R., Vianna, N., Chambers, J., Ray, D., Guerreiros, J.B., Lefebvre, P., Sternberg, L., Moreira, M., Barros, L., Ishida, F.Y., Tohlver, I., Belk, E., Kalif, K., Schwalbe, K., 2002. The effects of partial throughfall exclusion on canopy processes, aboveground production, and biogeochemistry of an Amazon forest. J. Geophys. Res. 107, 18.

Nobre, C.A., Sellers, P.J., Shukla, J., 1991. Amazonian deforestation and regional climate change. J. Climate 4, 957–988.

Oliveira, P.H.F., Artaxo, P., Pires, C., De Lucca, S., Procópio, A., Holben, B., Schafer, J., Cardoso, L.F., Wofsy, S.C., Rocha, H.R., 2007. The effects of biomass burning aerosols and clouds on the CO_2 flux in Amazonia. Tellus B 59, 338–349.

Oliveira, R.S., Dawson, T.E., Burgess, S.S.O., Nepstad, D.C., 2005. Hydraulic redistribution in three Amazonian trees. Oecologia 145, 354–363.

Papaioannou, G., Papanikolaou, N., Retalis, D., 1993. Relationships of photosynthetically active radiation and shortwave irradiance. Theor. Appl. Climatol. 48, 23–27.

Papale, D., Reichstein, M., Aubinet, M., Canfora, E., Bernhofer, C., Kutsch, W., Longdoz, B., Rambal, S., Valentini, R., Vesala, T., Yakir, D., 2006. Towards a standardized processing of net ecosystem exchange measured with eddy covariance technique: algorithms and uncertainty estimation. Biogeosciences 3, 571–583.

Peel, M.C., Finlayson, B.L., McMahon, T.A., 2007. Updated world map of the Köppen–Geiger climate classification. Hydrol. Earth Syst. Sci. 11, 1633–1644.

Pereira da Silva, R., dos Santos, J., Tribuzy, E.S., Chambers, J.Q., Nakamura, S., Higuchi, N., 2002. Diameter increment and growth patterns for individual tree growing in Central Amazon, Brazil. For. Ecol. Manage. 166, 295–301.

Potter, C., 2003. Continental-scale comparisons of terrestrial carbon sinks estimated from satellite data and ecosystem modeling 1982–1998. Global Planet. Change 39, 201–213.

Potter, C.S., Davidson, E.A., Klooster, S.A., Nepstad, D.C., De Negreiros, G.H., Brooks, V., 1998. Regional application of an ecosystem production model for studies of biogeochemistry in Brazilian Amazonia. Global Change Biol. 4, 315–333.

Restrepo-Coupe, N., Christoffersen, B., da Rocha, H.R., da Araujo, A.C., Borma, L.S., Cabral, O.M.R., de Camargo, P.B., Cardoso, F.L., da Costa, A.C.L., Fitzjarrald, D.R., Goulden, M.L., Hutyra, L.R., Kruijt, B., Maia, J.M.F., Malhi, Y.S., Manzi, A.O., Miller, S.D., Nobre, A.D., von Randow, C., da Sá, L.D.A., Sakai, R.K., Tota, J., Wofsy, S.C., Zanchi, F.B., Saleska, S.R., 2013. Gross ecosystem productivity seasonality in the tropics: issues posed by the absence of CO_2 profile measurements at eddy-flux systems (in preparation).

Rice, A.H., PYLE, E.H., Saleska, S.R., Hutyra, L.R., Palace, M., Keller, M., de Camargo, P.B., Portilho, K., Marques, D.F., Wofsy, S.C., 2004. Carbon balance and vegetation dynamics in an old-growth Amazonian forest. Ecol. Appl. 14, S55–S71.

Rosolem, R., Shuttleworth, W.J., de Gonçalves, L.G.G., 2008. Is the data collection period of the Large-Scale Biosphere-Atmosphere Experiment in Amazonia representative of long-term climatology? J. Geophys. Res. 113, 12.

Sakai, R.K., Fitzjarrald, D.R., Moraes, O.L.L., Staebler, R.M., Acevedo, O.C., Czikowsky, M.J., da Silva, R., Brait, E., Miranda, V., 2004. Land-use change effects on local energy, water, and carbon balances in an Amazonian agricultural field. Global Change Biol. 10, 895–907.

Saleska, S.R., Miller, S.D., Matross, D.M., 2003. Carbon in Amazon forests: unexpected seasonal fluxes and disturbance-induced losses. Science 302, 1554–1557.

Saleska, S.R., da Rocha, H.R., Kruijt, B., Nobre, A.D., 2009. Ecosystem carbon fluxes and Amazonian forest metabolism. In: Amazonia and Global Change. American Geophysical Union, Washington, DC.

Shuttleworth, W.J., 1988. Evaporation from Amazonian rainforest. Proc. R. Soc. Lond. B: Biol. Sci. 233, 321–346.

Sitch, S., Smith, B., Prentice, I.C., Arneth, A., Bondeau, A., Cramer, W., Kaplan, J.O., Levis, S., Lucht, W., Sykes, M.T., Thonicke, K., Venevsky, S., 2003. Evaluation of ecosystem dynamics, plant geography and terrestrial carbon cycling in the LPJ dynamic global vegetation model. Global Change Biol. 9, 161–185.

Sobrado, M.A., 1994. Leaf age effects on photosynthetic rate, transpiration rate and nitrogen content in a tropical dry forest. Physiol. Plant. 90, 210–215.

Sombroek, W., 2001. Spatial and temporal patterns of Amazon rainfall. Consequences for the planning of agricultural occupation and the protection of primary forests. Ambio 30, 388–396.

Souza Filho, J.D., da, C., Ribeiro, A., Costa, M.H., Cohen, J.C.P., 2005. Mecanismos de controle da variação sazonal da transpiração de uma floresta tropical no nordeste da amazônia. Acta Amaz, 35.

Stoy, P.C., Katul, G.G., Siqueira, M.B.S., Juang, J.-Y., Novick, K.A., Uebelherr, J.M., Oren, R., 2006. An evaluation of models for partitioning eddy covariance-measured net ecosystem exchange into photosynthesis and respiration. Agric. For. Meteorol. 141, 2–18.

Szeicz, G., 1974. Solar radiation for plant growth. J. Appl. Ecol. 11, 617–636.

Teixeira, W.G., Schroth, G., Marques, J.D., Huwe, B., 2003. Sampling and TDR probe insertion in the determination of the volumetric soil water content. Rev. Brasil. Ciência Solo 27, 576–581.

Thornton, P.E., Law, B.E., Gholz, H.L., Clark, K.L., Falge, E., Ellsworth, D.S., Goldstein, A.H., Monson, R.K., Hollinger, D., Falk, M., Chen, J., Sparks, J.P., 2002. Modeling and measuring the effects of disturbance history and climate on carbon and water budgets in evergreen needleleaf forests. Agric. For. Meteorol. 113, 185–222.

Tian, H., Melillo, J.M., Kicklighter, D.W., McGuire, A.D., Helfrich, J.V.K., Moore, B., Vorosmarty, C.J., 1998. Effect of interannual climate variability on carbon storage in Amazonian ecosystems. Nature 396, 664–667.

Tomasella, J., Hodnett, M.G., Cuartas, L.A., Nobre, A.D., Waterloo, M.J., Oliveira, S.M., 2007. The water balance of an Amazonian micro-catchment: the effect of interannual variability of rainfall on hydrological behaviour. Hydrol. Processes 22, 2133–2147.

von Randow, C., Manzi, A.O., Kruijt, B., de Oliveira, P.J., Zanchi, F.B., Silva, R.L., Hodnett, M.G., Gash, J.H.C., Elbers, J.A., Waterloo, M.J., Cardoso, F.L., Kabat, P., 2004. Comparative measurements and seasonal variations in energy and carbon exchange over forest and pasture in South West Amazonia. Theor. Appl. Climatol. 78, 5–26.

Werth, D., Avissar, R., 2002. The local and global effects of Amazon deforestation. J. Geophys. Res. 107, 8.

Wehr, R., Munger, J.W., Nelson, D.D., McManus, J.B., Zahniser, M.S., Wofsy, S.C., Saleska, S.R., 2013. Long-term eddy covariance measurements of the isotopic composition of the ecosystem-atmosphere exchange of CO_2 in a temperate forest. Agric. For. Meteoro, In press.

Wick, B., Veldkamp, E., De Mello, W.Z., Keller, M., Crill, P., 2005. Nitrous oxide fluxes and nitrogen cycling along a pasture chronosequence in Central Amazonia, Brazil. Biogeosci. Disc. 2, 499–535.

Wofsy, S., Goulden, M., Munger, J.W., 1993. Net exchange of CO_2 in a mid-latitude forest. Science 260, 1314–1317.

Wright, S.J., Van Schaik, C.P., 1994. Light and the phenology of tropical trees. Am. Naturalist 143, 192–199.

Xiao, X., Zhang, Q., Saleska, S., Hutyra, L., De Camargo, P., Wofsy, S., Frolking, S., Boles, S., Keller, M., Moore III, B., 2005. Satellite-based modeling of gross primary production in a seasonally moist tropical evergreen forest. Remote Sens. Environ. 94, 105–122.

Yuan, W., Liu, S., Zhou, G., Zhou, G., Tieszen, L.L., Baldocchi, D., Bernhofer, C., Gholz, H., Goldstein, A.H., Goulden, M.L., Hollinger, D.Y., Hu, Y., Law, B.E., Stoy, P.C., Vesala, T., Wofsy, S.C., 2007. Deriving a light use efficiency model from eddy covariance flux data for predicting daily gross primary production across biomes. Agric. For. Meteorol. 143, 189–207.

Zanchi, F.B., Waterloo, M.J., Aguiar, L.J.G., von Randow, C., Kruijt, B., Cardoso, F.L., Manzi, A.O., 2009. Estimate of the leaf area index (LAI) and biomass in pasture in the state of Rondônia – Brazil. Acta Amaz. 39, 335–347.